NACA

RESEARCH MEMORANDUM

THE EFFECT OF THICKNESS RATIO ON SECTION THRUST DISTRIBUTION AS DETERMINED FROM A STUDY OF WAKE SURVEYS OF THE NACA 4-(0)(03)-045 AND 4-(0)(08)-045 TWO-BLADE PROPELLERS UP TO FORWARD MACH NUMBERS OF 0.925

By Daniel E. Harrison and Joseph R. Milillo

Langley Aeronautical Laboratory
Langley Field, Va.

NATIONAL ADVISORY COMMITTEE
FOR AERONAUTICS

WASHINGTON
April 5, 1951

NATIONAL ADVISORY COMMITTEE FOR AERONAUTICS

RESEARCH MEMORANDUM

THE EFFECT OF THICKNESS RATIO ON SECTION THRUST DISTRIBUTION AS DETERMINED FROM A STUDY OF WAKE SURVEYS OF THE NACA 4-(0)(03)-045 AND 4-(0)(08)-045 TWO-BLADE PROPELLERS UP TO FORWARD MACH NUMBERS OF 0.925

By Daniel E. Harrison and Joseph R. Mililo

SUMMARY

Tests of the NACA 4-(0)(03)-045 and the NACA 4-(0)(08)-045 two-blade propellers were conducted in the Langley 8-foot high-speed tunnel for blade angles from 40° to 65° through a Mach number range up to 0.925.

The results show that changes in thrust loading due to compressibility effects were much smaller for the NACA 4-(0)(03)-045 thin-blade propeller than for the NACA 4-(0)(08)-045 thick-blade propeller. At maximum-efficiency conditions, the thrust loading on the outboard sections increased sufficiently with Mach number, for the highest Mach numbers tested, to produce higher integrated values of thrust coefficient than were obtained at subcritical Mach numbers. This trend indicates that the lift coefficient at which maximum L/D is obtained at supercritical speeds is greater than at subcritical speeds. The thin propeller delayed the forward Mach number at which compressibility effects occur at least 0.05 as compared to the thicker blade for all blade angles tested.

INTRODUCTION

The effects of thickness ratio on propeller aerodynamic characteristics as determined from an investigation of the NACA 4-(0)(03)-045 and the NACA 4-(0)(08)-045 propellers were reported in references 1 and 2. In these papers, only the force-test results were presented. Wake-survey measurements were also obtained in conjunction with the force tests to determine the thrust distributions on the two propellers. It is

the purpose of the present paper to give the thrust distributions in coefficient form and to show how these distributions are altered by the effects of thickness ratio.

The tests reported herein were conducted in the Langley 8-foot high-speed tunnel using the same apparatus and methods as those described in reference 3.

SYMBOLS

b	blade width, feet
C_T	thrust coefficient $\left(\frac{T}{\rho n^2 D^4}\right)$
D	propeller diameter, feet
b/D	blade-width ratio
h	maximum thickness of blade section, feet
h/b	blade-thickness ratio
J	advance ratio $\left(\frac{V_o}{nD}\right)$
M	tunnel-datum (forward) Mach number (tunnel Mach number uncorrected for tunnel-wall constraint)
M_t	helical-tip Mach number $\left(M\sqrt{1+\left(\frac{\pi}{J}\right)^2}\right)$
n	propeller rotational speed, revolutions per second
q	dynamic pressure $\left(\frac{\rho V^2}{2}\right)$
R	propeller-tip radius, feet
r	blade-section radius, feet
r_w	wake-section radius, feet
T	thrust, pounds

[redacted]

T_c	thrust disk-loading coefficient $\left(\frac{T}{2qD^2}\right)$
V	tunnel-datum velocity (tunnel velocity uncorrected for tunnel-wall constraint), feet per second
V_o	equivalent free-air velocity (tunnel-datum velocity corrected for tunnel-wall constraint), feet per second
x_w	wake station $\left(r_w/R\right)$
ρ	air density, slugs per cubic foot
β	section blade angle, degrees
$\beta_{0.75R}$	blade angle at 0.75 radius, degrees
η_{max}	maximum efficiency
$\frac{dC_T}{dx_w}$	section thrust coefficient

APPARATUS, METHODS, AND TESTS

The tests reported herein were conducted in the Langley 8-foot high-speed tunnel using the same apparatus and methods as those described in reference 3. A sketch of the 800-horsepower dynamometer as installed in the tunnel is included as figure 1.

Propellers.- Two two-blade propellers with 4-foot diameters were used in this investigation. Each propeller was designed as a two-blade configuration having the same blade loading to produce minimum induced losses (profile drag assumed equal to zero) at a nominal blade angle of 60° at the 0.7-radius station and at an advance ratio of 3.36. Symmetrical NACA 16-series propeller sections were used all along the blades. These propellers have the same plan form, approximately the same pitch distribution, and differ essentially only in thickness ratio. The thin-blade propeller, NACA 4-(0)(03)-045, has approximately the same thickness at the root as the thick-blade propeller, NACA 4-(0)(08)-045, but tapers very rapidly along the blade.

The designation numbers have the following meaning. The number of the first group is the diameter in feet; the second number, in parentheses,

[redacted]

is the design lift coefficient (in tenths) of the blade section at the 0.7-radius station; the third number, in parentheses, is the thickness ratio of the blade section at the 0.7-radius station; and the last number is the blade solidity expressed as a ratio of the blade chord at the 0.7-radius station to the circumference of the circle having a radius 0.7 of the propeller-tip radius. A photograph of the blades is shown in figure 2, and the blade-form curves are given in figure 3.

Survey rakes.- Section thrust coefficients were computed from static- and total-pressure measurements in the slipstream of the propeller. The total-pressure measurements were obtained by means of the rakes shown in figure 1. The rake struts had a maximum thickness ratio of 10 percent perpendicular to the leading edge and were swept back at an angle of 45°. These factors contributed to keeping the tunnel-choking Mach number at as high a level as possible. The total pressure was measured in a plane 17 inches downstream from the center line of the propeller. An inclined manometer board was used to measure total pressure; the angle of inclination was such that 3 inches of measurement were obtained for each inch of vertical height of the manometer fluid.

Thrust, torque, rotational speed, and slipstream pressures were measured throughout the operating range of the propellers. The propeller were tested with the blade angle fixed and the rotational speed was varied over a range for each tunnel Mach number. Data were taken at blade angles as low as 20°, but these are not included because of inaccuracies in measuring the smaller values of total-pressure rise in the slipstream. The range of blade angles presented for each forward Mach number is given in the following tables:

Forward Mach number M	NACA 4-(0)(03)-045 propeller blade angle of 0.75-radius station, $\beta_{0.75R}$ (deg)				
0.23	40				
.35	40				
.43	40				
.53	40	50			
.60		50	55	60	
.65		50	55	60	
.70		50	55	60	65
.75		50	55	60	65
.80		50	55	60	65
.85		50	55	60	65
.90		50	55	60	65
.925		50	55	60	65

Forward Mach number M	NACA 4-(0)(08)-045 propeller blade angle at 0.75-radius station, $\beta_{0.75R}$ (deg)			
0.53	50			
.60	50	55		
.65	50	55	60	
.70	50	55	60	65
.75	50	55	60	65
.80	50	55	60	65
.85		55	60	65
.90		55	60	65
.925		55	60	65

REDUCTION OF DATA

Section thrust coefficients were computed from measurements of the static- and total-pressure changes in the wake of the propeller. The simplified method presented in reference 4, which does not require the measurement of temperatures in the slipstream, was the method used to reduce the data presented herein.

The slipstream radius r_w is assumed equal to the blade-section radius r.

With the propeller operating, it was found that the variation of static pressure measured radially outward from the dynamometer barrel was not enough to change appreciably the thrust distribution along the blade. Therefore, the static pressure, as used, was obtained by an orifice located on the dynamometer barrel in the plane of the rakes.

The advance ratio was corrected for the effect of tunnel-wall constraint by use of the ratio of free-air velocity to the tunnel-datum velocity as a function of thrust disk-loading coefficient and tunnel-datum Mach number as presented in figure 4 (reference 3).

ACCURACY OF RESULTS

Section-thrust-coefficient values are not presented in the curves for radial stations inboard of the $x_w = 0.4$. These points were not presented because of the scatter of the data measured by the survey

[redacted]

equipment. This scatter was present both with and without the propeller installed in the test setup and therefore was caused by the erratic nature of the basic flow about the spinner gap and not by the propeller. However, the section thrust curves were extrapolated to the spinner location (x_w = 0.271). Other section-thrust-coefficient values omitted from the curves were due to faulty total-pressure tubes.

The thrust coefficients as obtained from the wake-survey data presented herein agree with the force-test data within ±7 percent. The wake-survey values are to be used to show the load distribution of the propellers qualitatively and not quantitatively. The data have not been corrected for rotational losses in the slipstream which, in general, would reduce the integrated thrust-coefficient values by approximately 4 percent. It is to be noted that this correction does not change appreciably the shape of the load-distribution curve along the blade.

RESULTS AND DISCUSSION

The basic section-thrust-coefficient curves for the NACA 4-(0)(03)-045 propeller are shown in figure 5 for $\beta_{0.75R} = 40^\circ$ to 65° through the Mach number and advance-ratio ranges tested. Similar curves for the NACA 4-(0)(08)-045 propeller for $\beta_{0.75R} = 50^\circ$ to 65° are presented as figure 6. The force-test characteristic curves corresponding to these section-thrust-coefficient curves have previously been presented in references 1 and 2.

Effect of forward Mach number on thrust distribution.- Figure 7 shows the effect of forward Mach number on the thrust distribution at maximum efficiency for the NACA 4-(0)(03)-045 propeller for $\beta_{0.75R} = 50^\circ$, 55°, 60°, and 65°. Each set of curves is identified by the corresponding Mach numbers and advance ratio.

In general, the shape of the thrust-distribution curves remains relatively constant at low speeds. As the tip-section speeds become supercritical, the onset of shock and separation results in a loss in lift (decreased lift-curve slope). This, coupled with an increase in drag, results in a lower thrust loading on the outboard sections. As the forward Mach number is further increased, the thrust loading on the outboard sections is greatly increased. This is primarily a result of an increase in angle of attack as evidenced by the decrease in advance ratio. It is believed that the increase in thrust loading is also due to a slight increase in the lift-curve slope for these sections.

[redacted]

The foregoing observations are in agreement with results obtained from wind-tunnel tests of wings at transonic and low supersonic speeds. At subcritical speeds, section drag is little affected by Mach number, and lift coefficient increases with increasing Mach number approximately in accordance with the Prandtl-Glauert relation. At supercritical section speeds up to Mach number 1.0, a mixed flow, partly supersonic and partly subsonic, takes place on the airfoil which results in a rapid increase in drag and a simultaneous loss of lift. At low supersonic speeds, pure supersonic flow covers the entire airfoil (except at the leading edge); drag coefficient, though high, does not continue to increase with speed; and lift coefficient increases with increasing Mach number. This type of airfoil behavior is reflected in the variation of section thrust coefficient with Mach number. At subcritical speeds thrust coefficient increases slowly with increasing Mach number. At higher forward speed for conditions where a portion of the blade operates at supercritical section speeds, a local drop in the values of section thrust coefficient indicates the drag rise and loss of lift associated with transonic operation. The high values of section thrust coefficient attained on the outboard sections at high speed reflect the improved operation of the blade sections at supersonic speeds.

The efficiency of a propeller at supercritical speeds is governed largely by the lift-drag ratio of the blade sections. At maximum efficiency, the thrust loading on the outboard sections increased sufficiently, for the highest Mach numbers tested, to produce higher integrated values of thrust coefficient than were obtained at subcritical Mach numbers. This indicates that the lift coefficient at which maximum L/D is obtained at supercritical speeds is greater than at subcritical speeds. The increase in lift coefficient is primarily due to the increase in angle of attack at the high Mach numbers. Since the outboard sections of the propeller blade are more efficient than the inboard sections at the higher Mach numbers, it would be expected that the rise in thrust loading would be greater at the outer sections.

The effects of forward Mach number on maximum efficiency have been reported in references 1 and 2 for the NACA 4-(0)(03)-045 and NACA 4-(0)(08)-045 propellers. The changes in maximum efficiency with forward Mach number show good correlation with the changes in thrust loading with Mach number shown in figures 7 and 8. The force data presented in figure 9 show that the maximum efficiency for the NACA 4-(0)(03)-045 propeller at $\beta = 60^\circ$ remains relatively constant up to a Mach number of 0.80. The thrust loading shown in figure 7 for the NACA 4-(0)(03)-045 propeller also remains the same up to a Mach number of 0.80. When the maximum efficiency decreases appreciably ($M = 0.85$), the thrust loading changes on the propeller sections. The same comparison of the changes in force data and wake-survey data with forward Mach number can be made for all blade angles tested.

[redacted]

Effect of thickness ratio.- The effect of thickness ratio on thrust distribution at maximum efficiency is shown in figure 10 by comparing the curves of the NACA 4-(0)(03)-045 and the NACA 4-(0)(08)-045 propellers at $\beta_{0.75R} = 55^\circ$. The changes in thrust loading with forward Mach number are much smaller for the NACA 4-(0)(03)-045 thin-blade propeller than for the NACA 4-(0)(08)-045 thick-blade propeller. This occurrence would be expected since the magnitude of lift losses due to compressibility effects decreases with decreasing thickness ratios. It can be seen that the thick blade began to experience compressibility effects at a forward Mach number of 0.75, as compared to the thin blade which began to experience compressibility effects at a forward Mach number of 0.80.

A comparison of the thrust-distribution curves is presented in figure 11 for the NACA 4-(0)(03)-045 and the NACA 4-(0)(08)-045 propellers at constant advance ratio for $\beta_{0.75R} = 60^\circ$. The advance ratio was chosen to correspond nearly to the subcritical maximum-efficiency operating condition for both propellers. The thrust coefficients for the thin blade were higher than those for the thick blade throughout the test Mach number range. The changes in thrust coefficients for the thick blade were more pronounced than those for the thin blade. The figure clearly shows that the thick blade began losing thrust loading at $M = 0.75$; whereas, for the thin blade, the losses are so small and occur so gradually that it is difficult to say at which forward Mach number the losses begin. The force-test (constant advance ratio) results presented in figure 12 show that the thrust coefficient for the thick blade starts to decrease at $M = 0.75$, whereas the thrust coefficient for the thin blade starts to decrease at 0.80 Mach number. This shows that compressibility effects were delayed at least 0.05 in forward Mach number by the use of very thin sections.

CONCLUSIONS

Tests of the NACA 4-(0)(03)-045 and NACA 4-(0)(08)-045 two-blade propellers conducted in the Langley 8-foot high-speed tunnel for blade angles between 40° and 65° and through a forward Mach number range up to 0.925 indicated the following results:

1. At maximum efficiency, the changes in thrust loading due to compressibility effects were much smaller for the NACA 4-(0)(03)-045 thin-blade propeller than for the NACA 4-(0)(08)-045 thick-blade propeller.

2. At maximum efficiency, the thrust loading on the outboard sections increased sufficiently with Mach number, for the highest Mach numbers tested, to produce higher values of thrust coefficient than

were obtained at subcritical Mach numbers. This trend indicates that the lift coefficient at which maximum L/D is obtained at supercritical speeds is much greater than at subcritical speeds. This effect was less pronounced for the NACA 4-(0)(03)-045 propeller than for the NACA 4-(0)(08)-045 propeller.

3. Comparison of the thrust coefficients of the test propellers at constant advance ratio indicates larger thrust loadings for the thin sections than for the thick sections.

4. The thin propeller delayed the forward Mach number at which compressibility effects occur at least 0.05 as compared to the thicker blade for all blade angles tested.

Langley Aeronautical Laboratory
National Advisory Committee for Aeronautics
Langley Field, Va.

REFERENCES

1. Carmel, Melvin M., and Milillo, Joseph R.: Investigation of the NACA 4-(0)(03)-045 Two-Blade Propeller at Forward Mach Numbers to 0.925. NACA RM L50A31a, 1950.

2. Delano, James B., and Carmel, Melvin M.: Investigation of the NACA 4-(0)(03)-045 and NACA 4-(0)(08)-045 Two-Blade Propellers at Forward Mach Numbers to 0.925. NACA RM L9L06a, 1950.

3. Delano, James B., and Carmel, Melvin M.: Investigation of the NACA 4-(5)(08)-03 Two-Blade Propeller at Forward Mach Numbers to 0.925. NACA RM L9G06a, 1949.

4. Baals, Donald D., and Mourhess, Mary J.: Numerical Evaluation of the Wake-Survey Equations for Subsonic Flow Including the Effect of Energy Addition. NACA ARR L5H27, 1945.

[redacted]

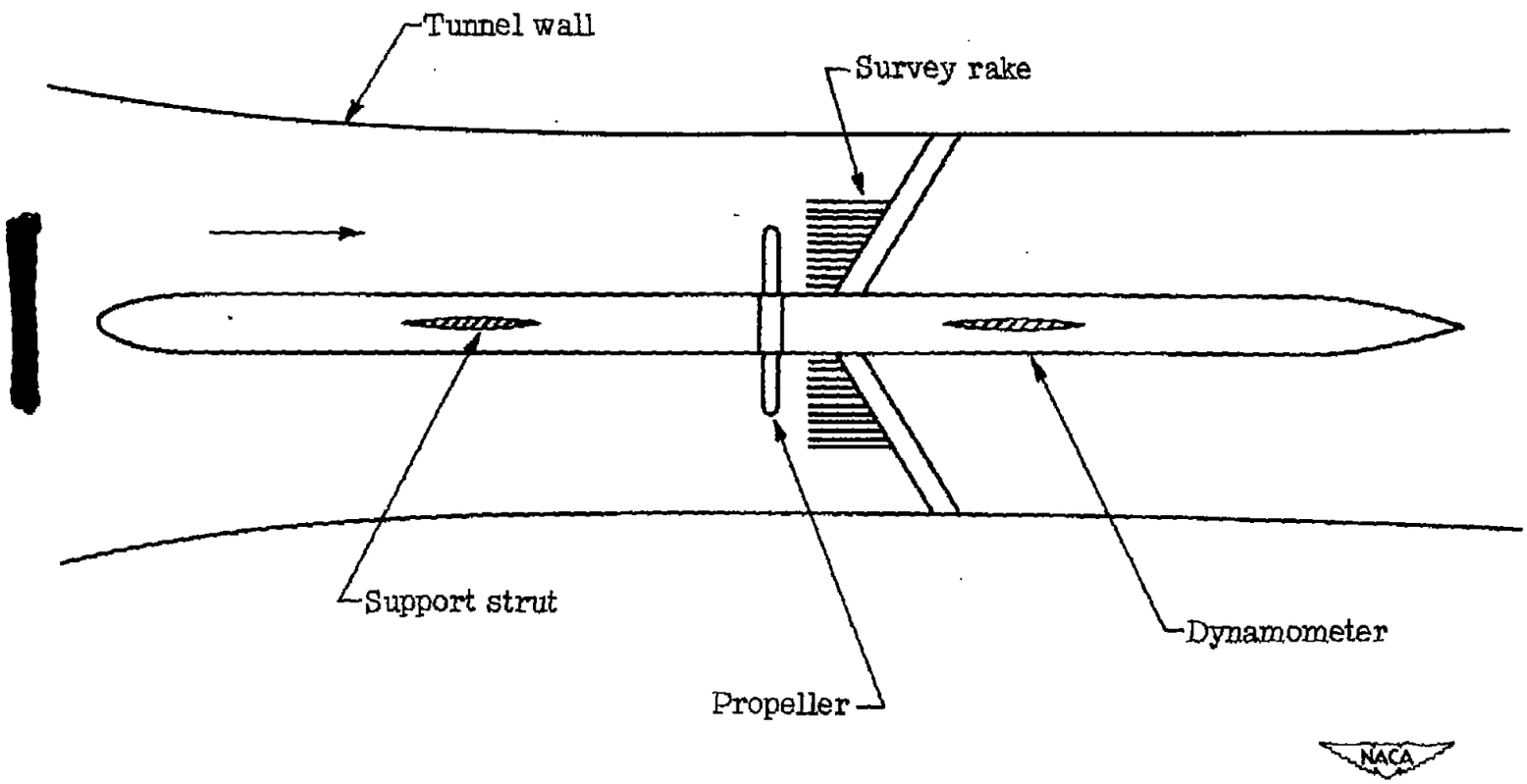

Figure 1.- Test apparatus.

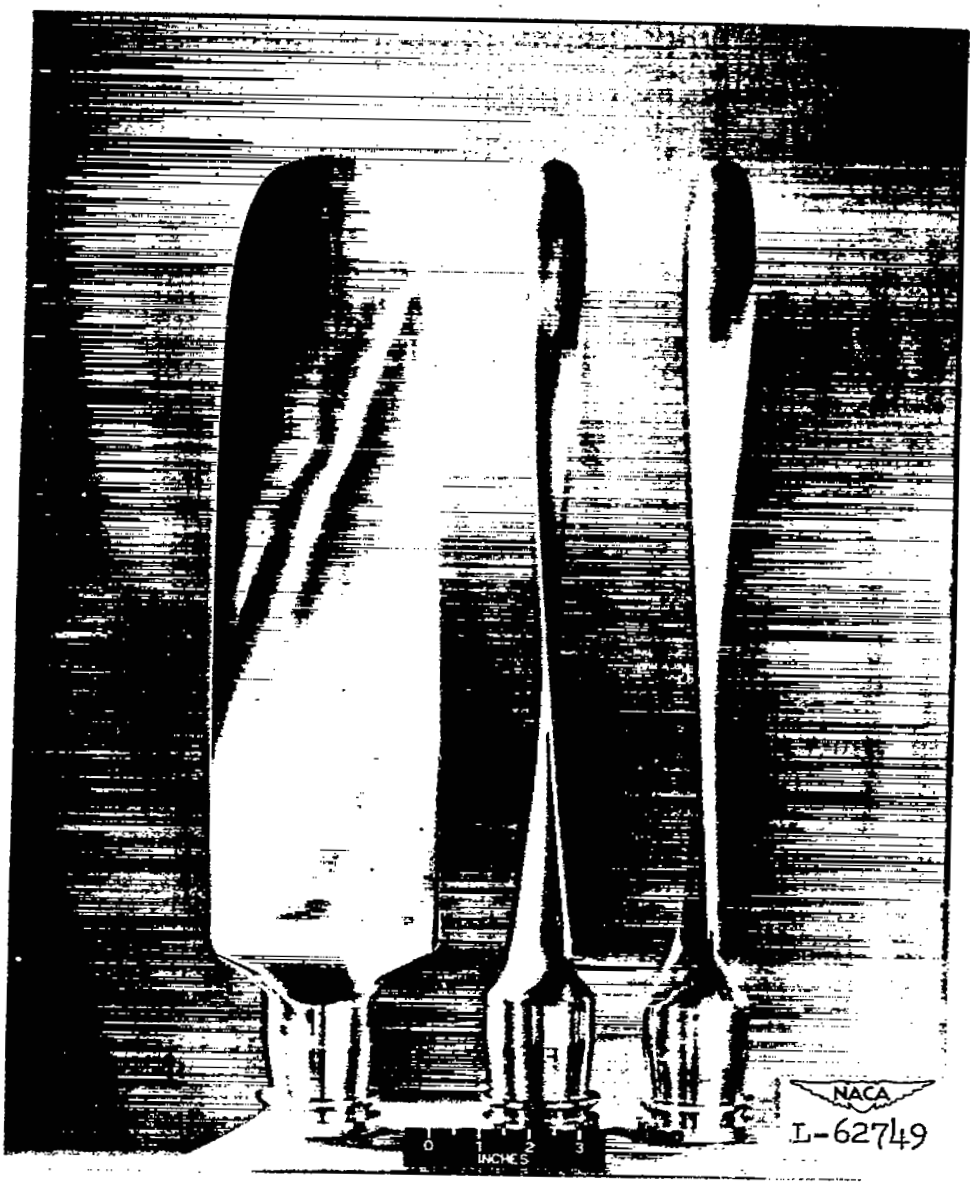

4-(0)(03)-045 4-(0)(03)-045 4-(0)(08)-045
4-(0)(08)-045

Figure 2.- Photograph of NACA 4-(0)(03)-045 and 4-(0)(08)-045 propellers.

[redacted]

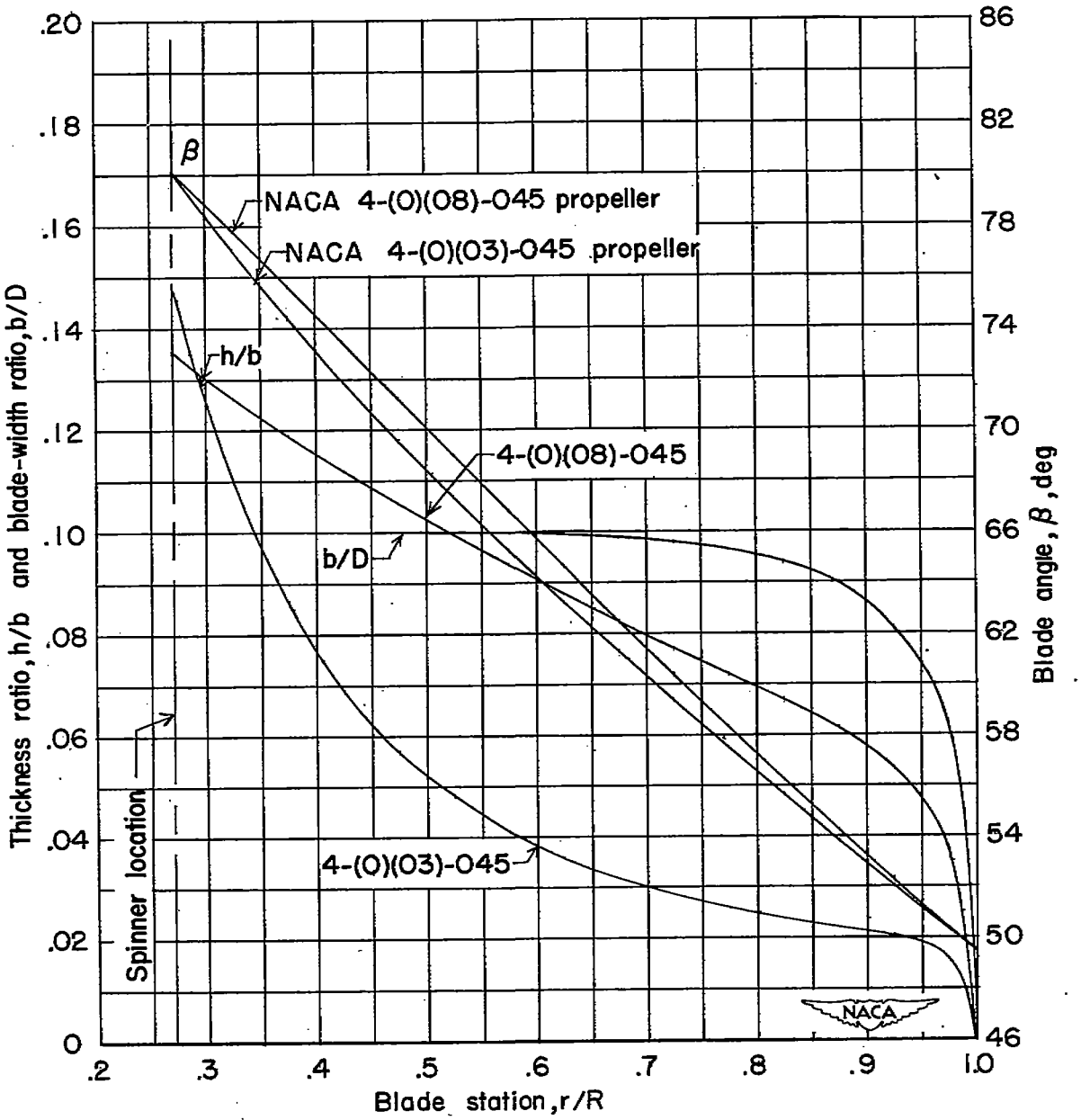

Figure 3.- NACA 4-(0)(03)-045 and NACA 4-(0)(08)-045 propeller blade-form curves.

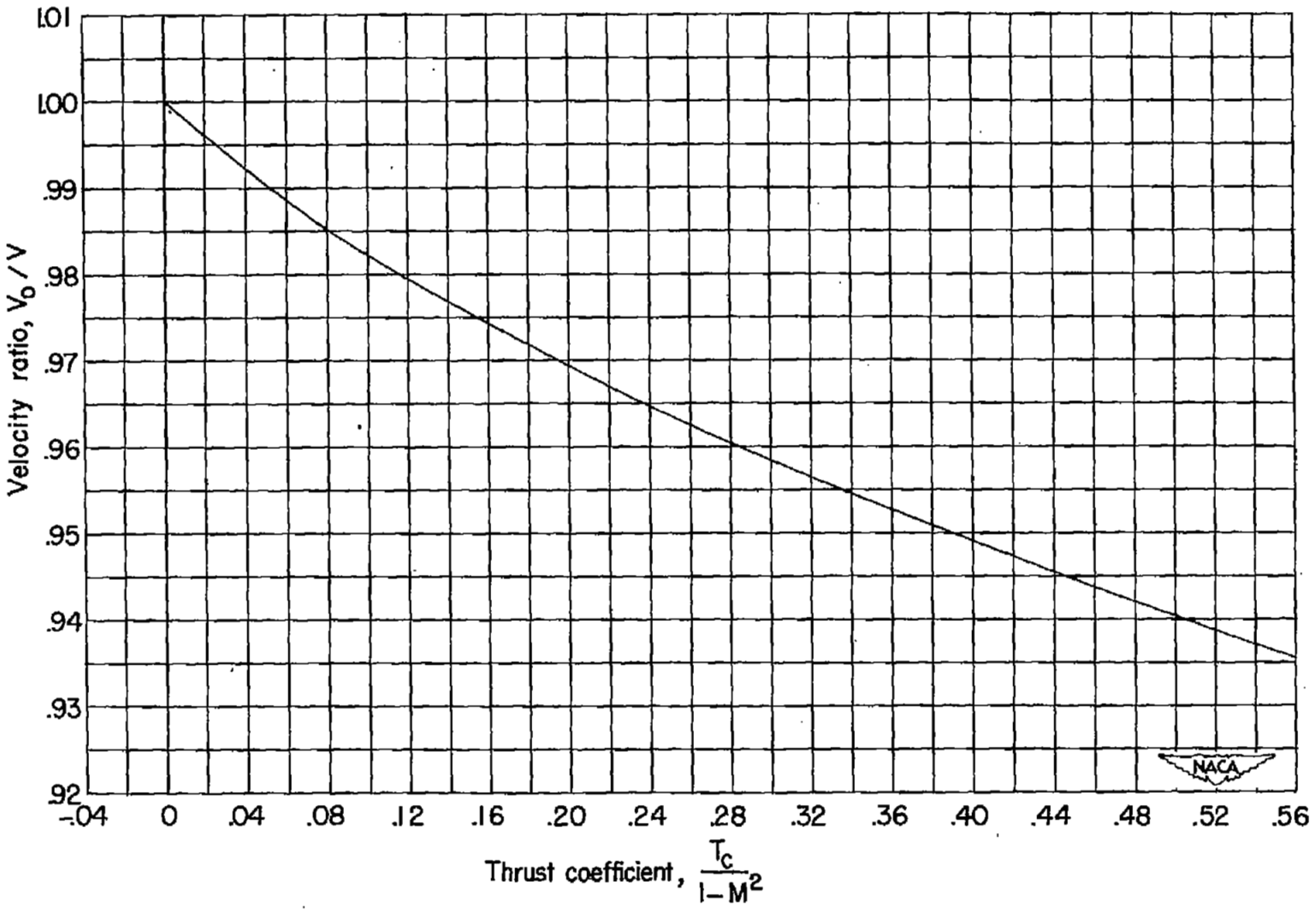

Figure 4.- Tunnel-wall-interference correction for 4-foot-diameter propeller in Langley 8-foot high-speed tunnel.

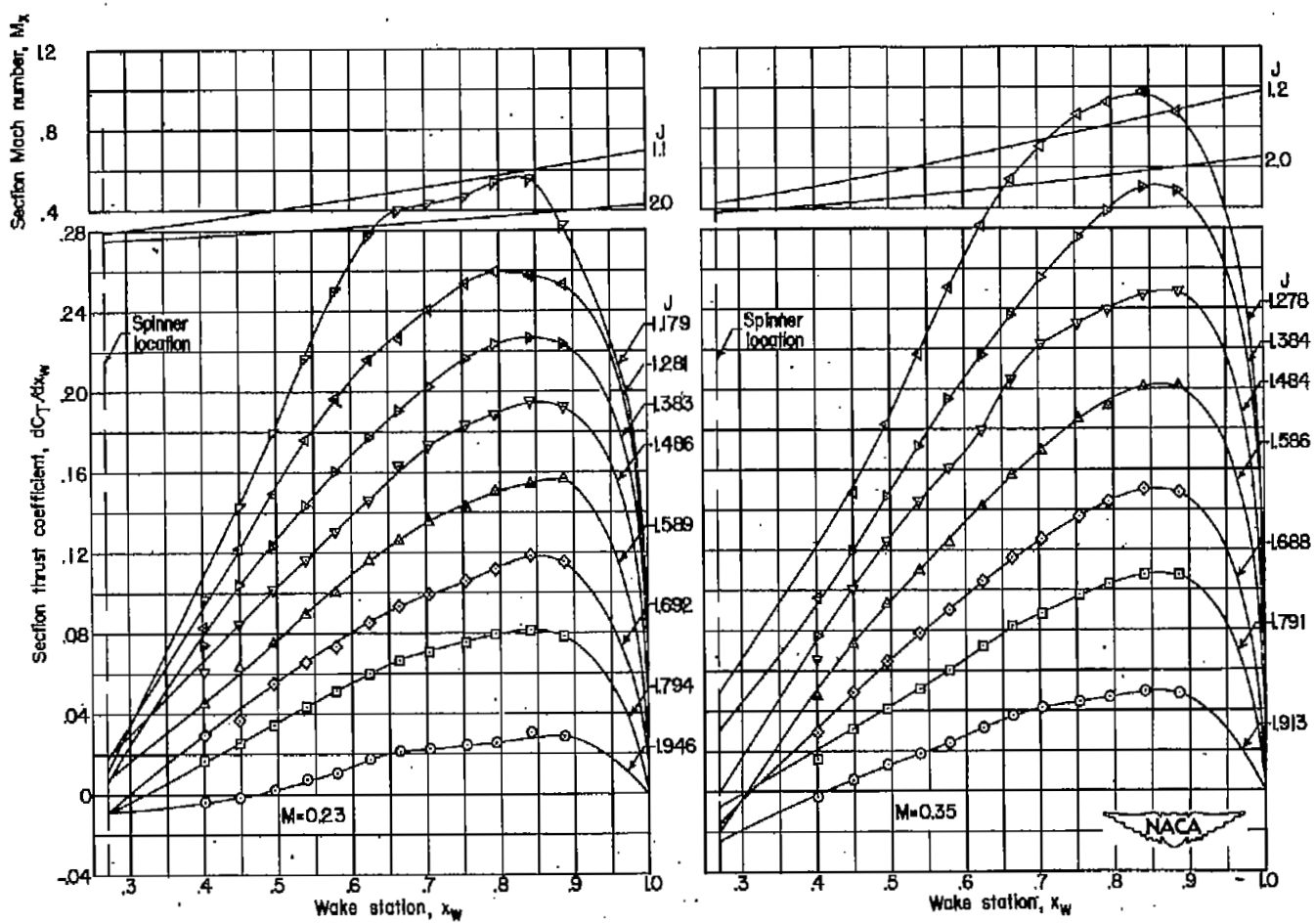

(a) $\beta_{0.75R} = 40^\circ$.

Figure 5.- Basic section-thrust-coefficient curves for NACA 4-(0)(03)-045 propeller.

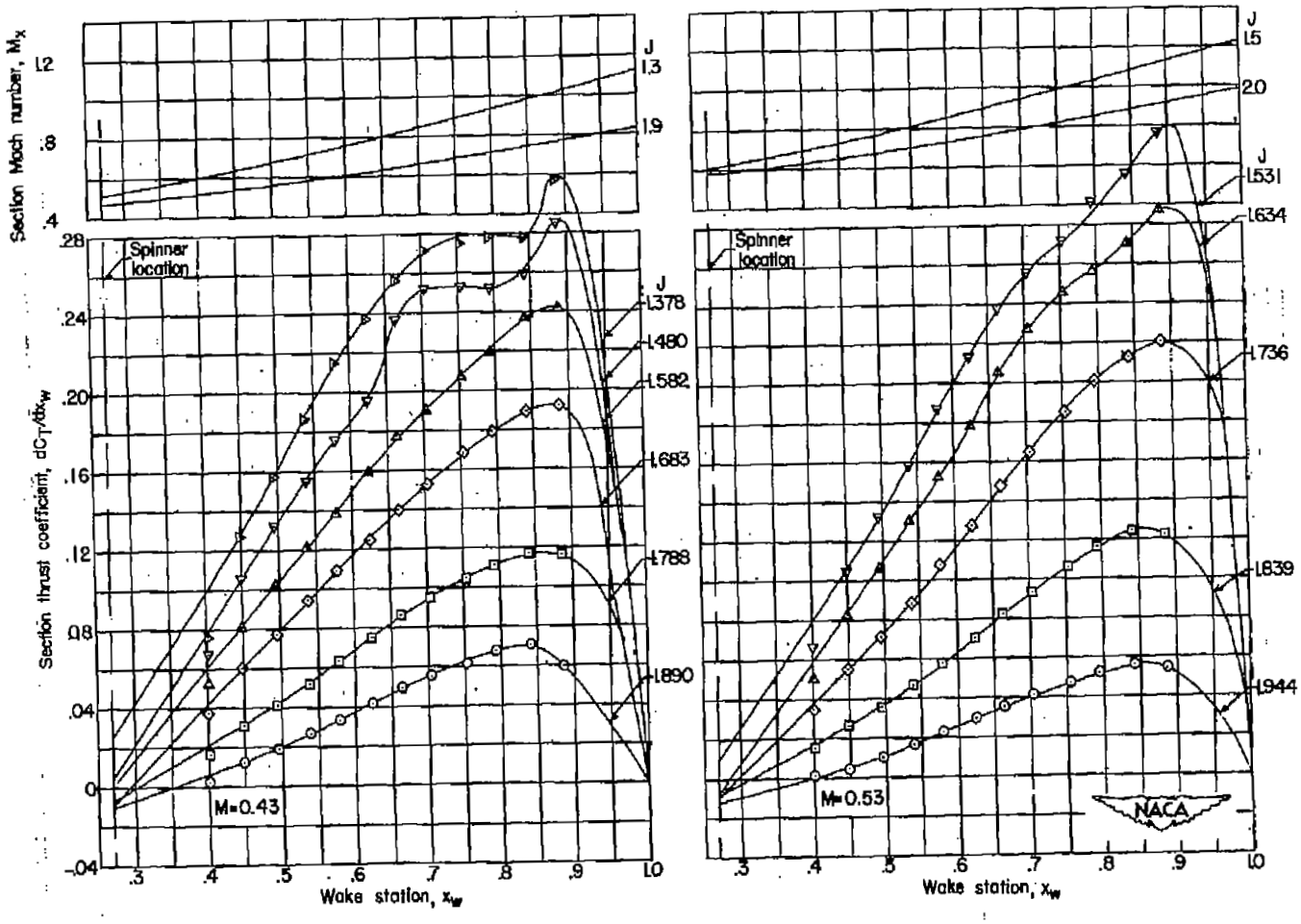

(a) Concluded. $\beta_{0.75R} = 40°$.

Figure 5.- Continued.

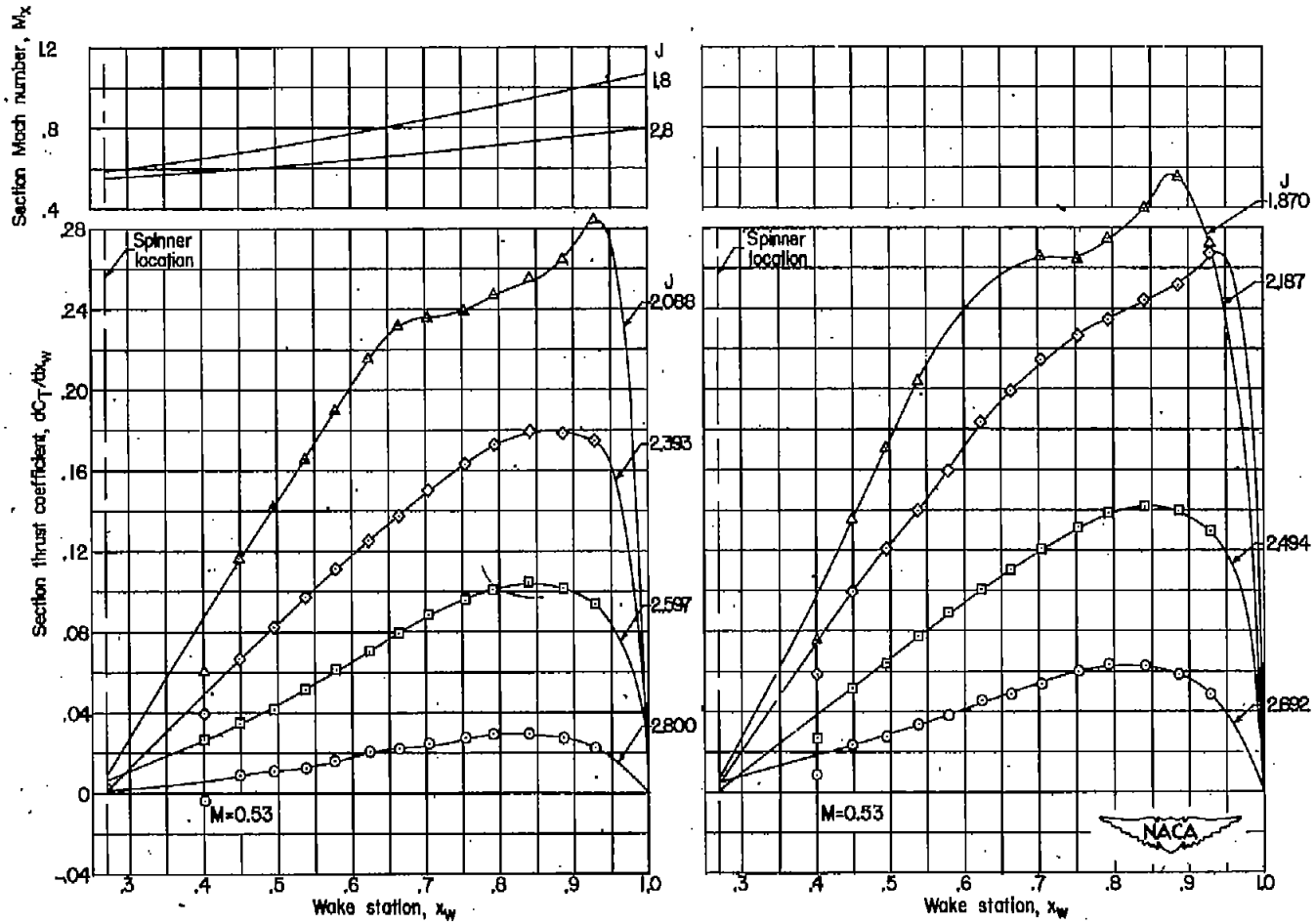

(b) $\beta_{0.75R} = 50^\circ$.

Figure 5.- Continued.

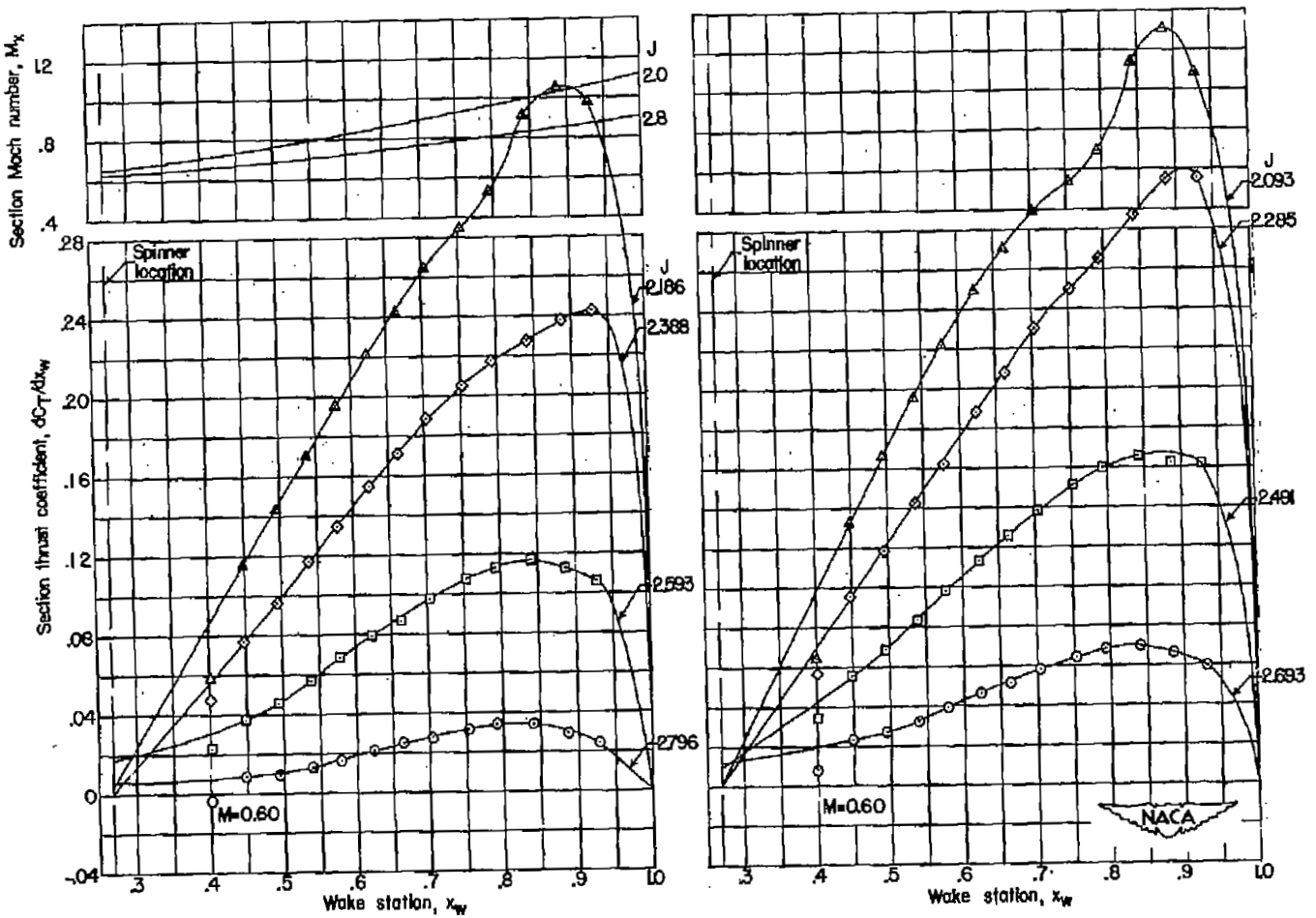

(b) Continued. $\beta_{0.75R} = 50°$.

Figure 5.- Continued.

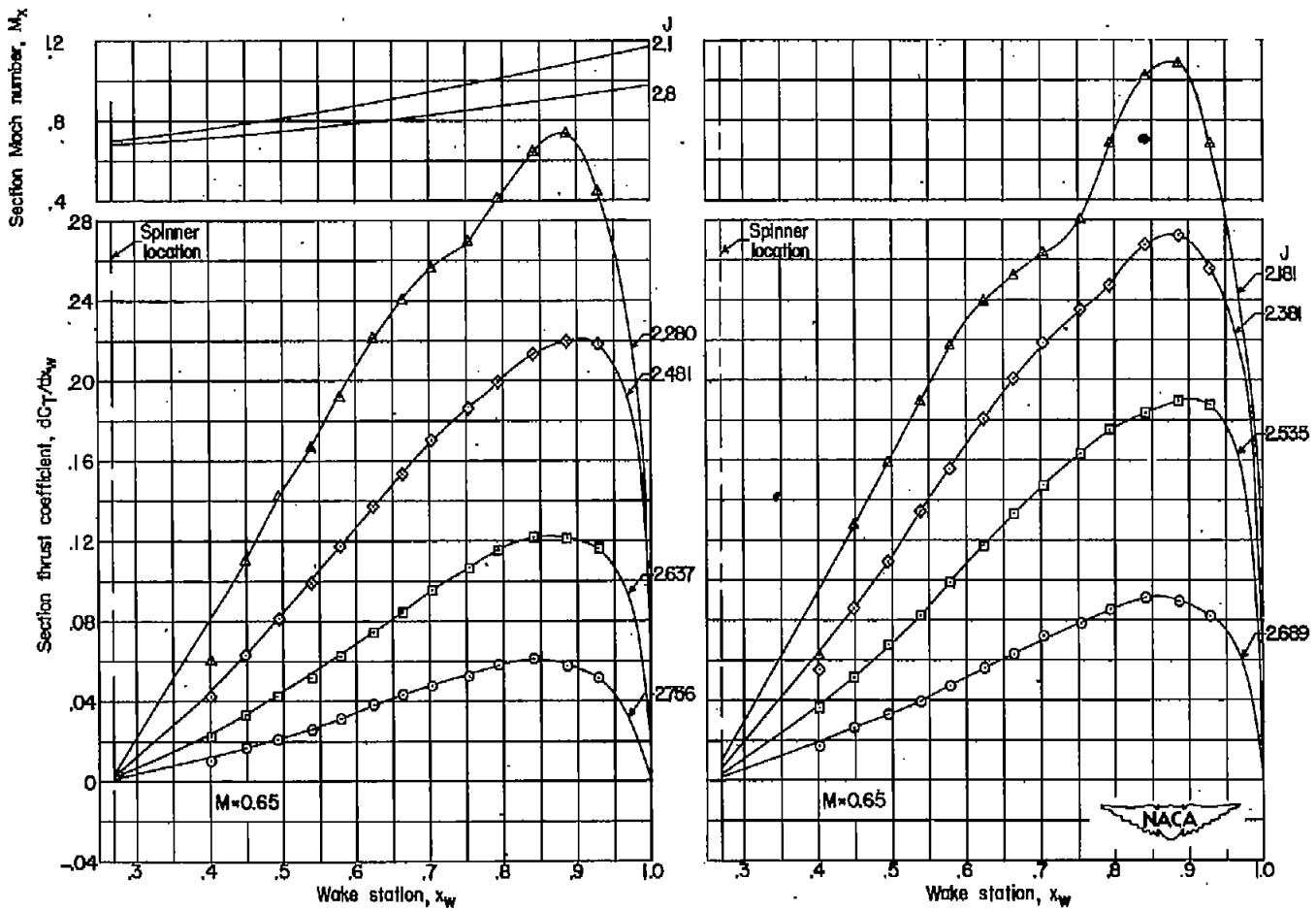

(b) Continued. $\beta_{0.75R} = 50^{\circ}$.

Figure 5.- Continued.

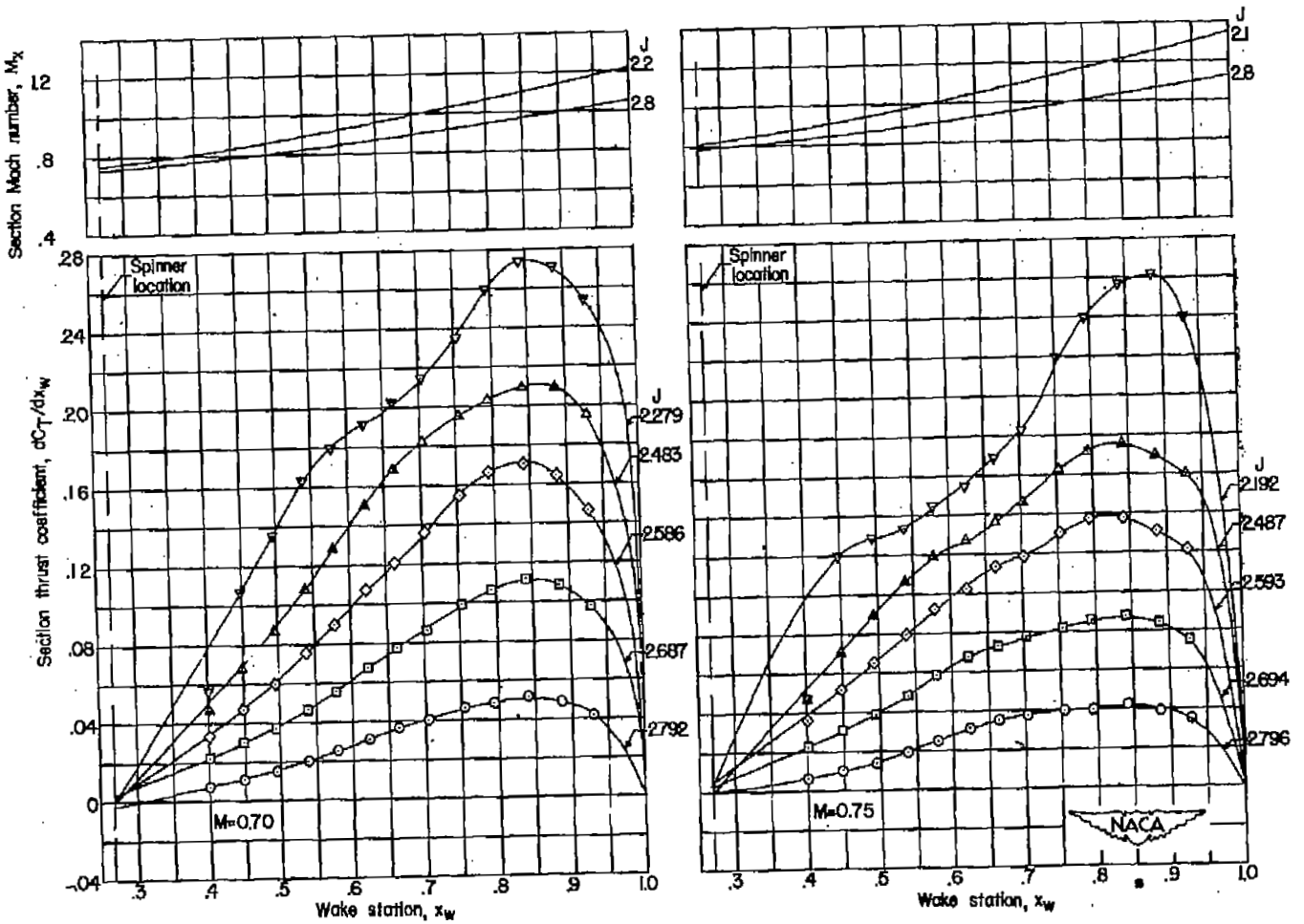

(b) Continued. $\beta_{0.75R} = 50°$.

Figure 5.- Continued.

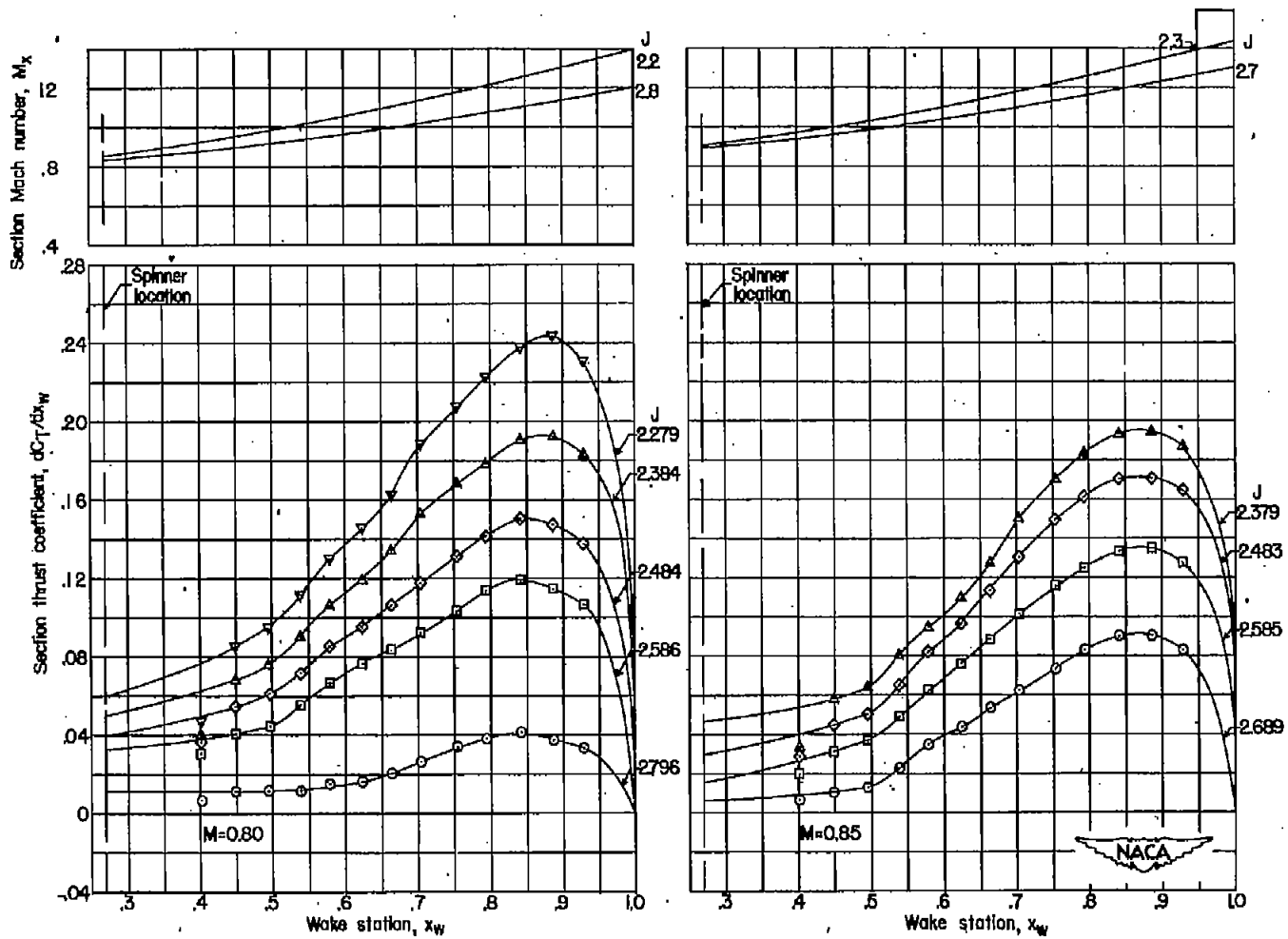

(b) Continued. $\beta_{0.75R} = 50^\circ$.

Figure 5.- Continued.

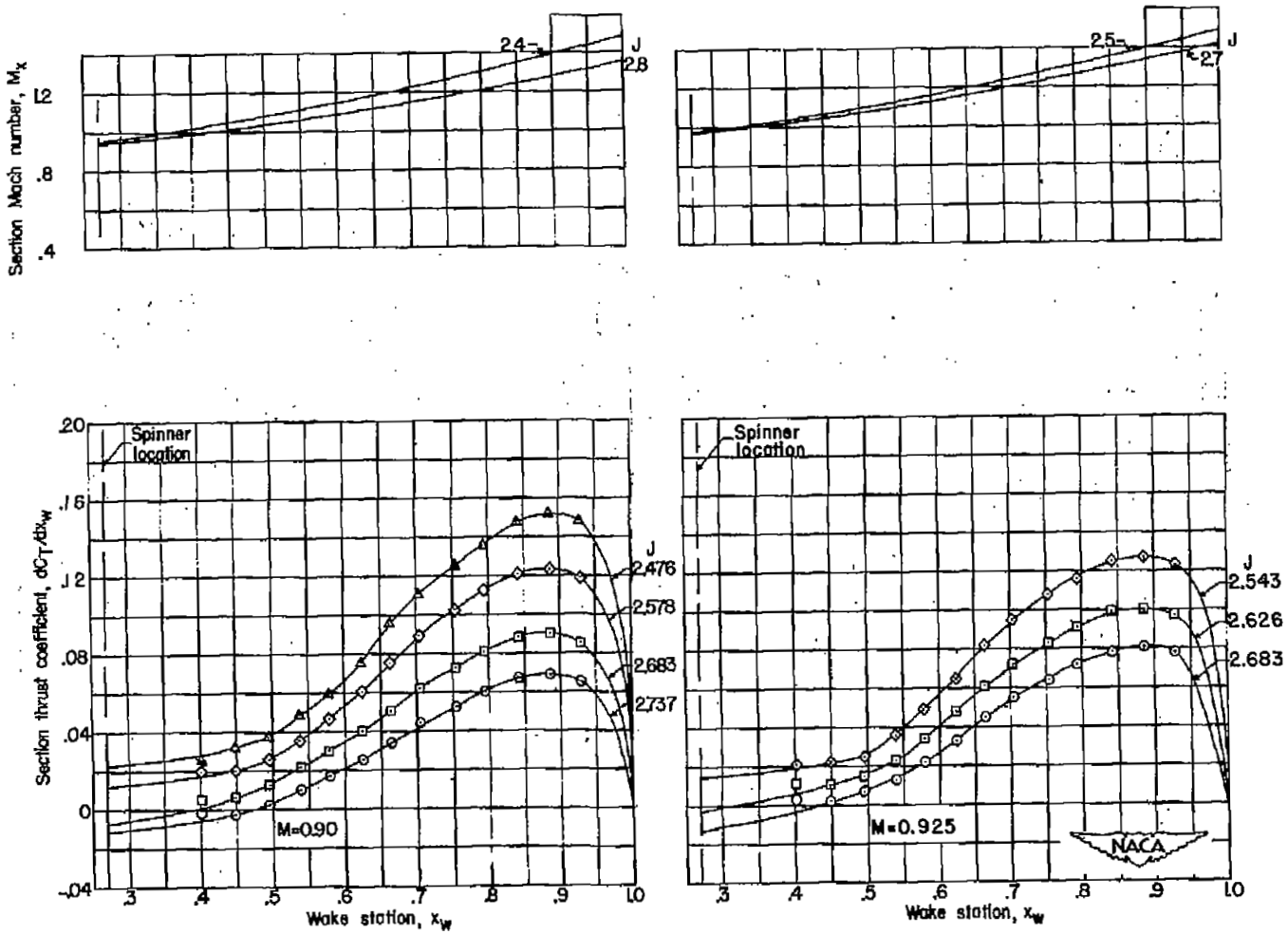

(b) Concluded. $\beta_{0.75R} = 50^{\circ}$.

Figure 5.- Continued.

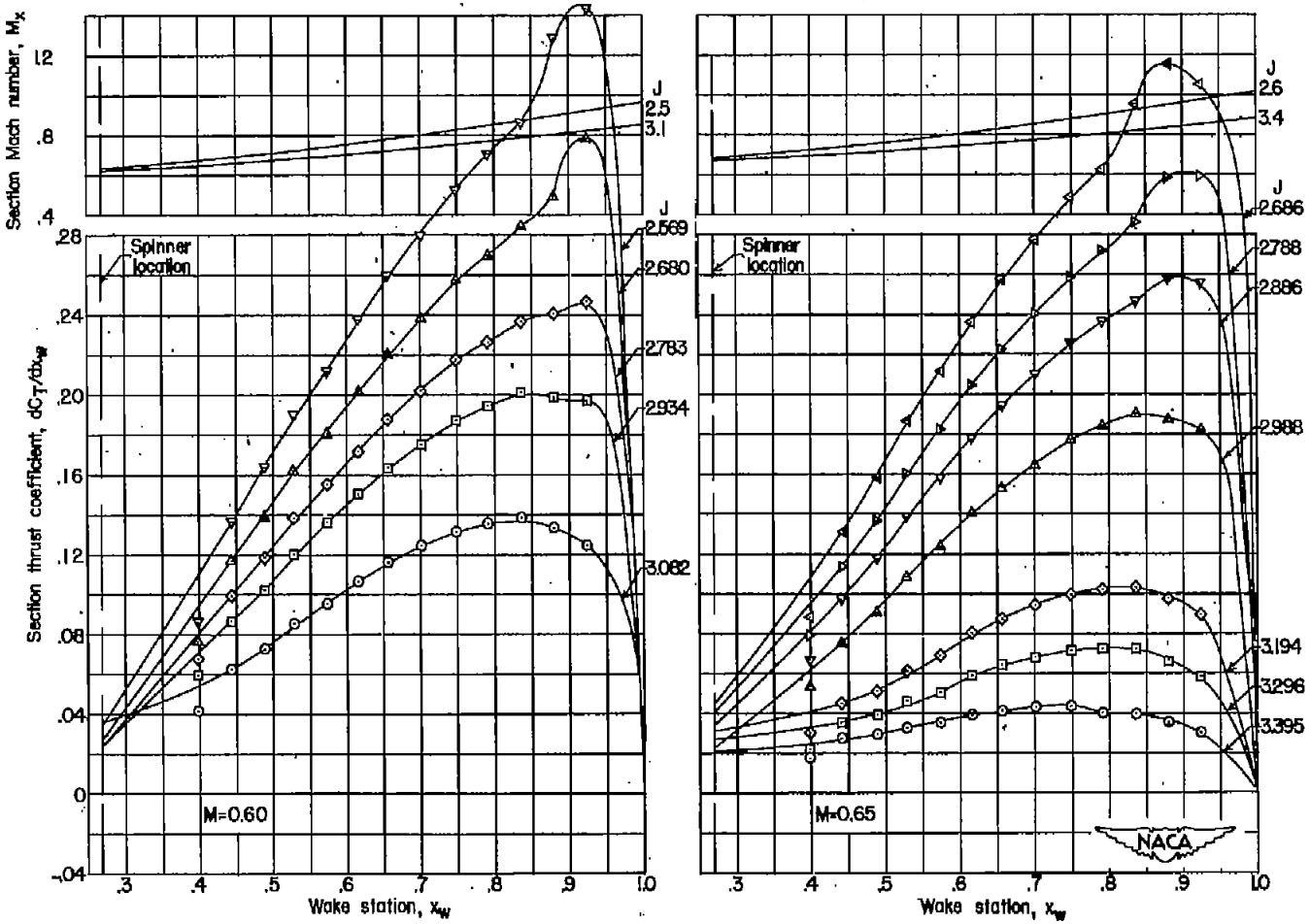

(c) $\beta_{0.75R} = 55^{\circ}$.

Figure 5.- Continued.

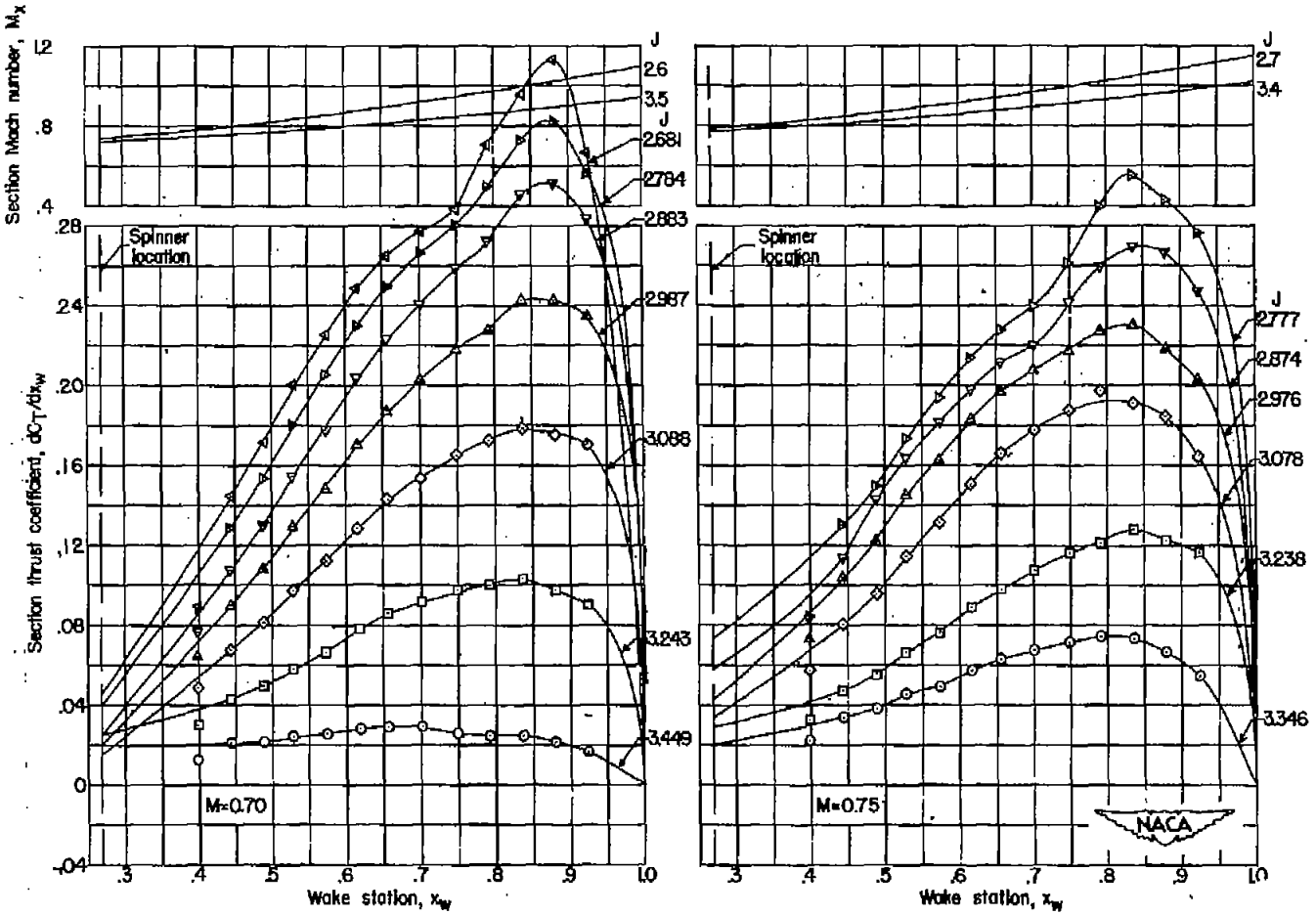

(c) Continued. $\beta_{0.75R} = 55^{\circ}$.

Figure 5.- Continued.

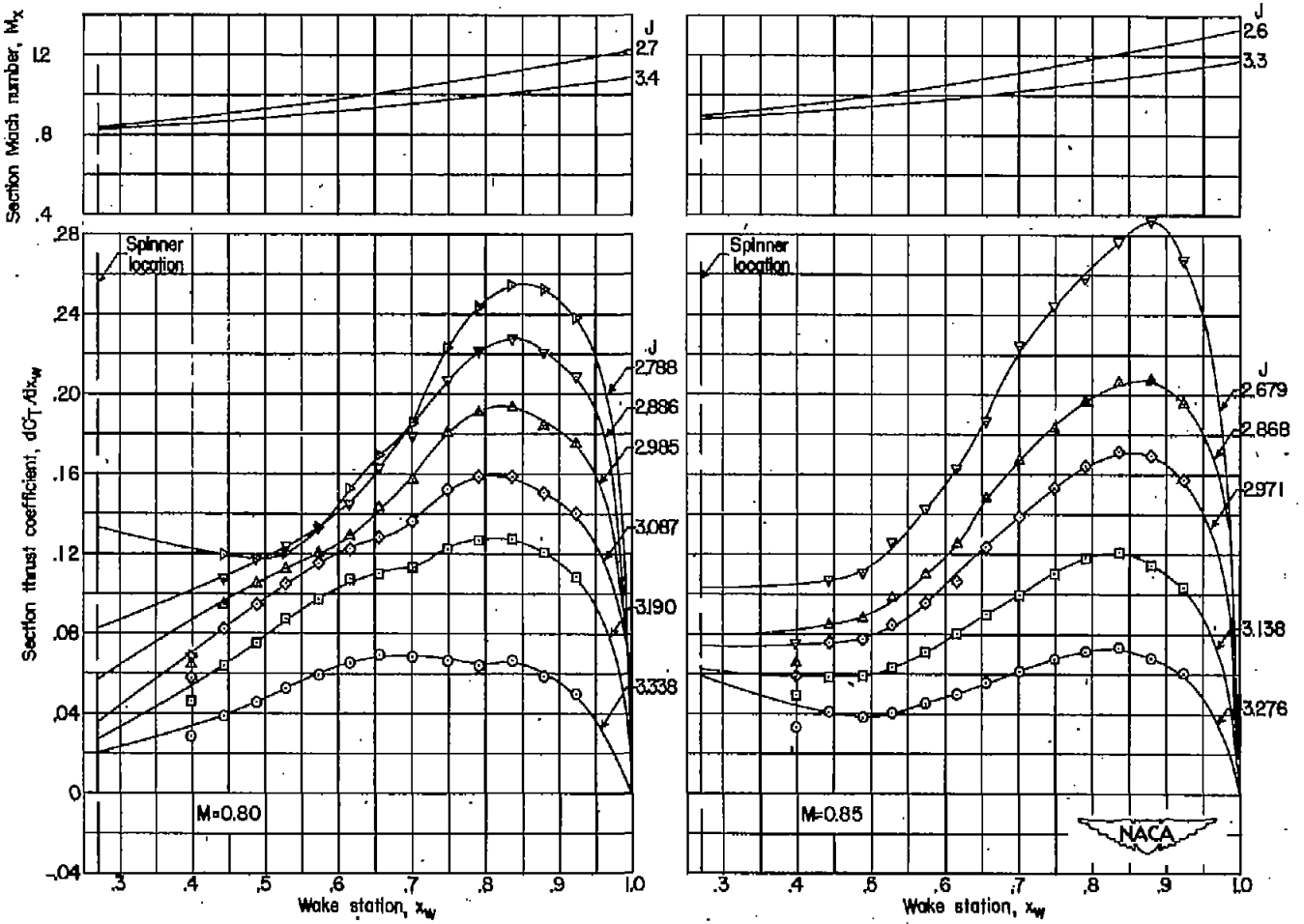

(c) Continued. $\beta_{0.75R} = 55°$.

Figure 5.- Continued.

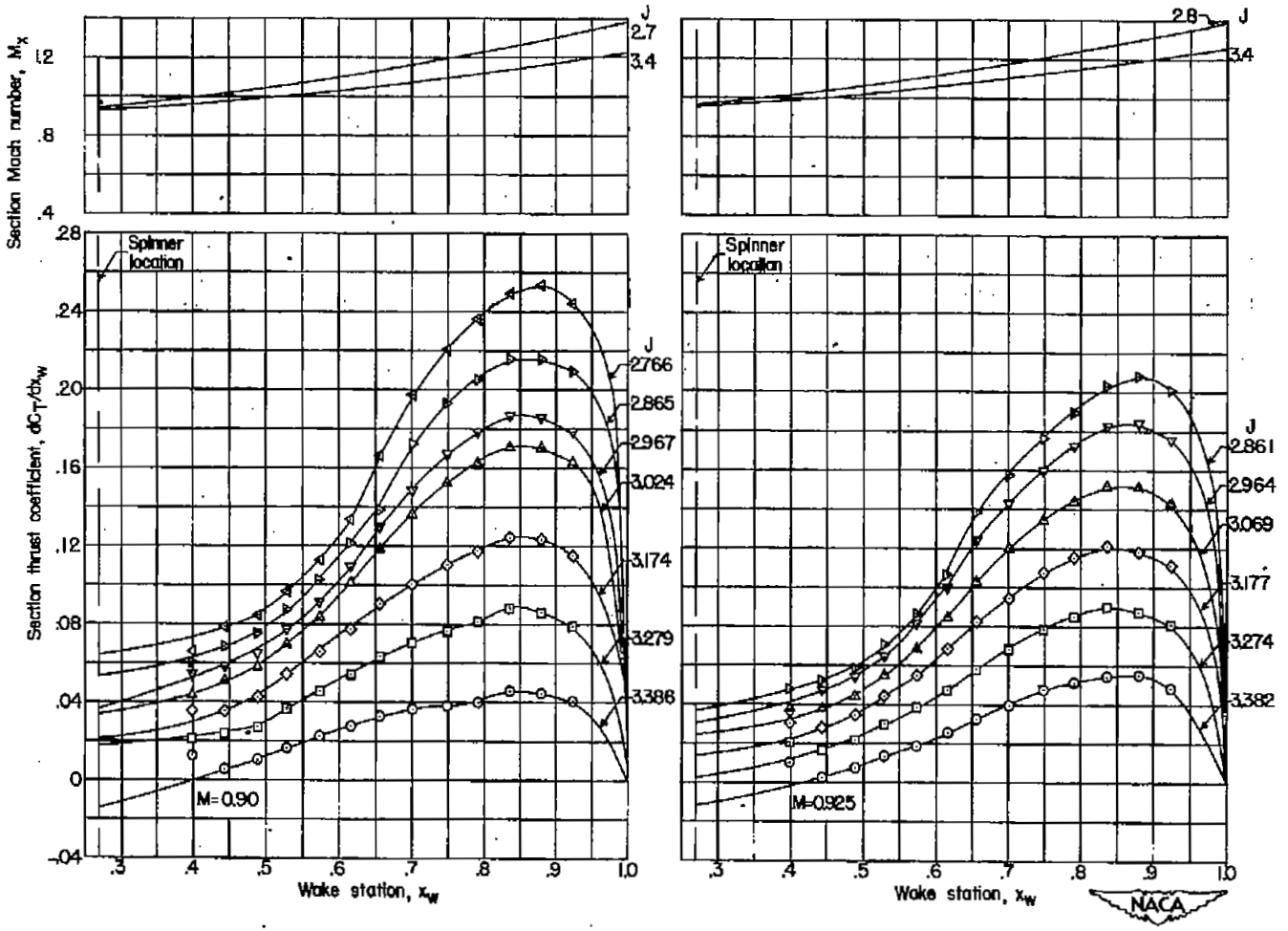

(c) Concluded. $\beta_{0.75R} = 55^{\circ}$.

Figure 5.- Continued.

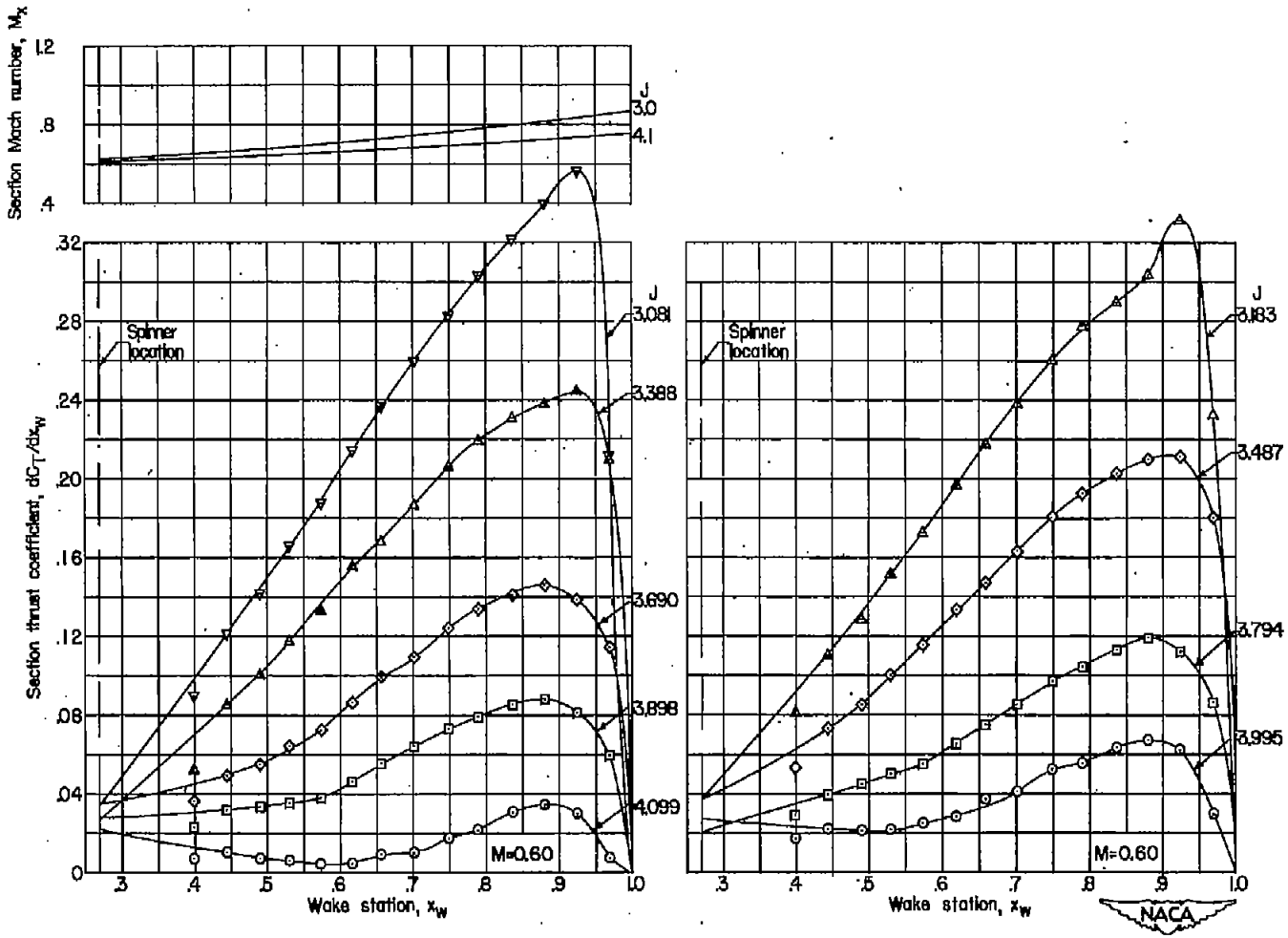

(d) $\beta_{0.75R} = 60°$.

Figure 5.- Continued.

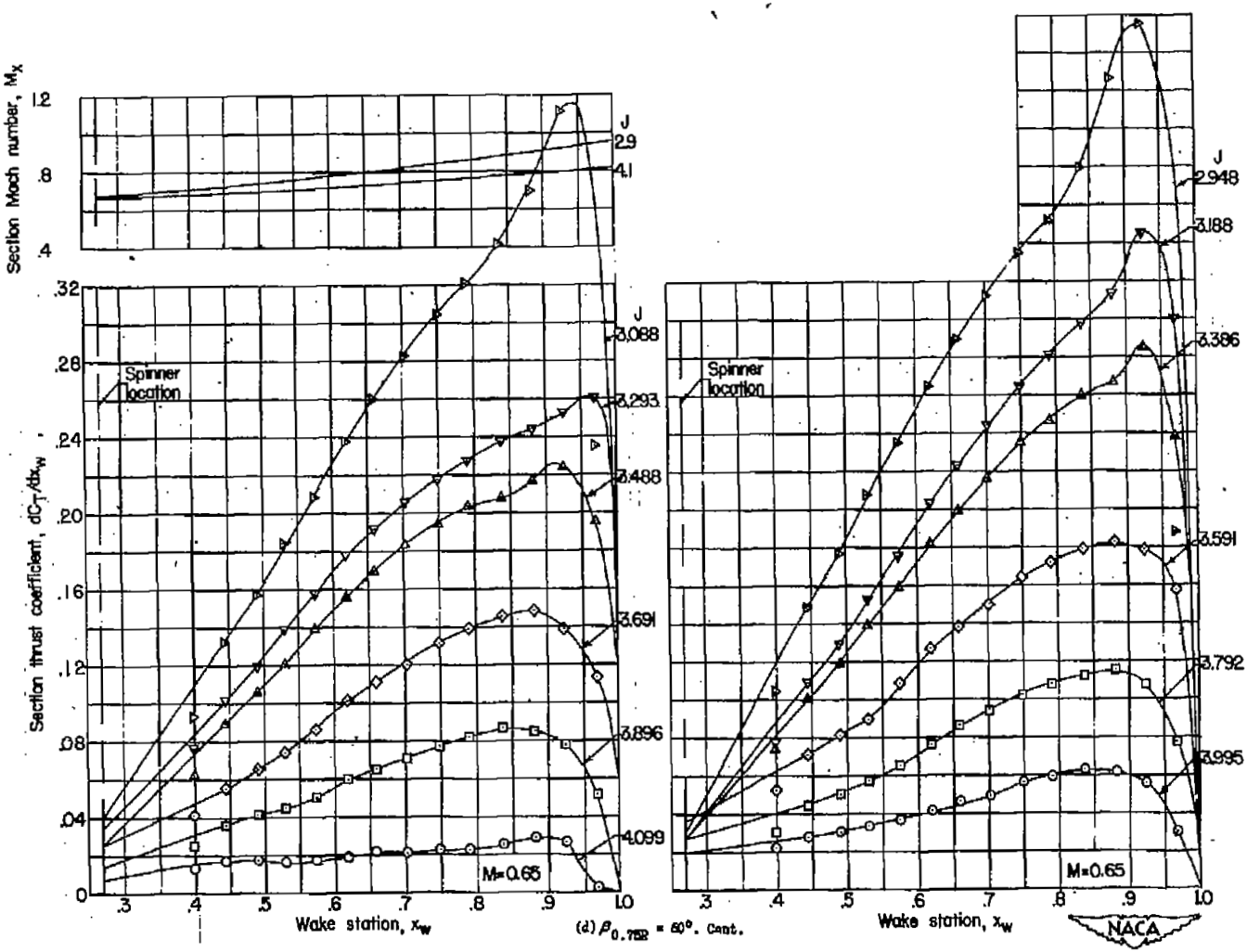

(d) Continued. $\beta_{0.75R} = 60°$.

Figure 5.- Continued.

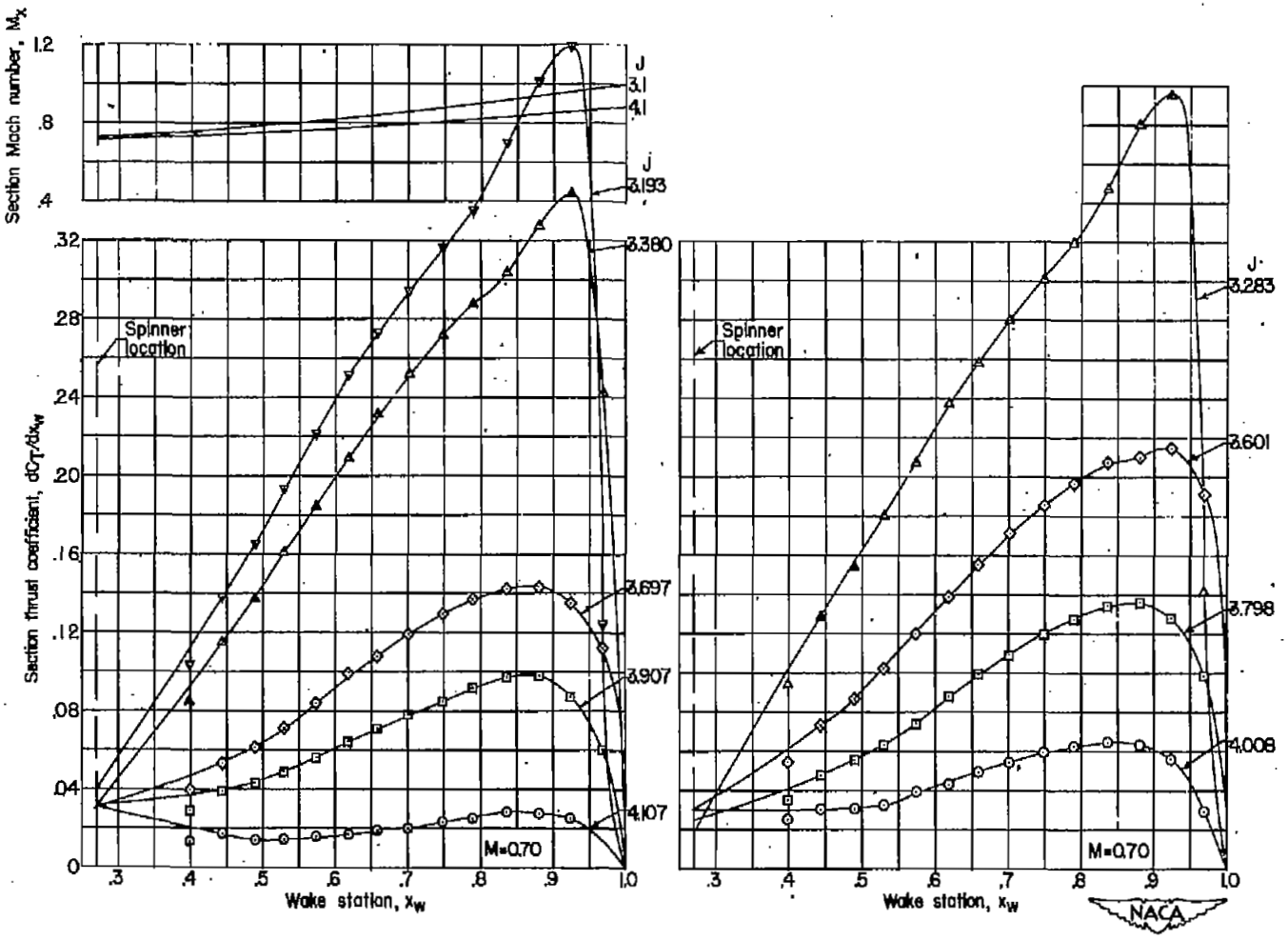

(d) Continued. $\beta_{0.75R} = 60^\circ$.

Figure 5.- Continued.

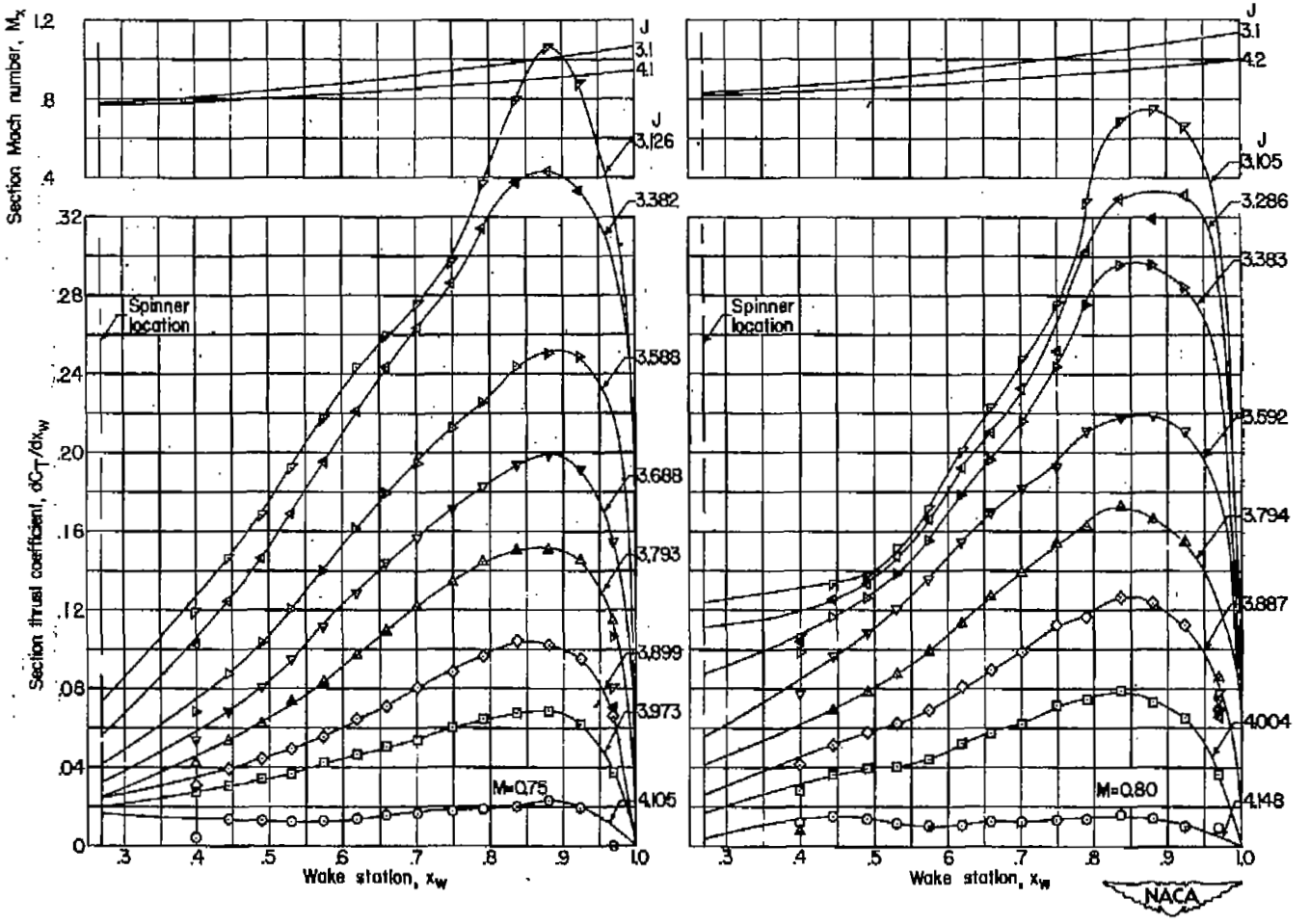

(d) Continued. $\beta_{0.75R} = 60^\circ$.

Figure 5.- Continued.

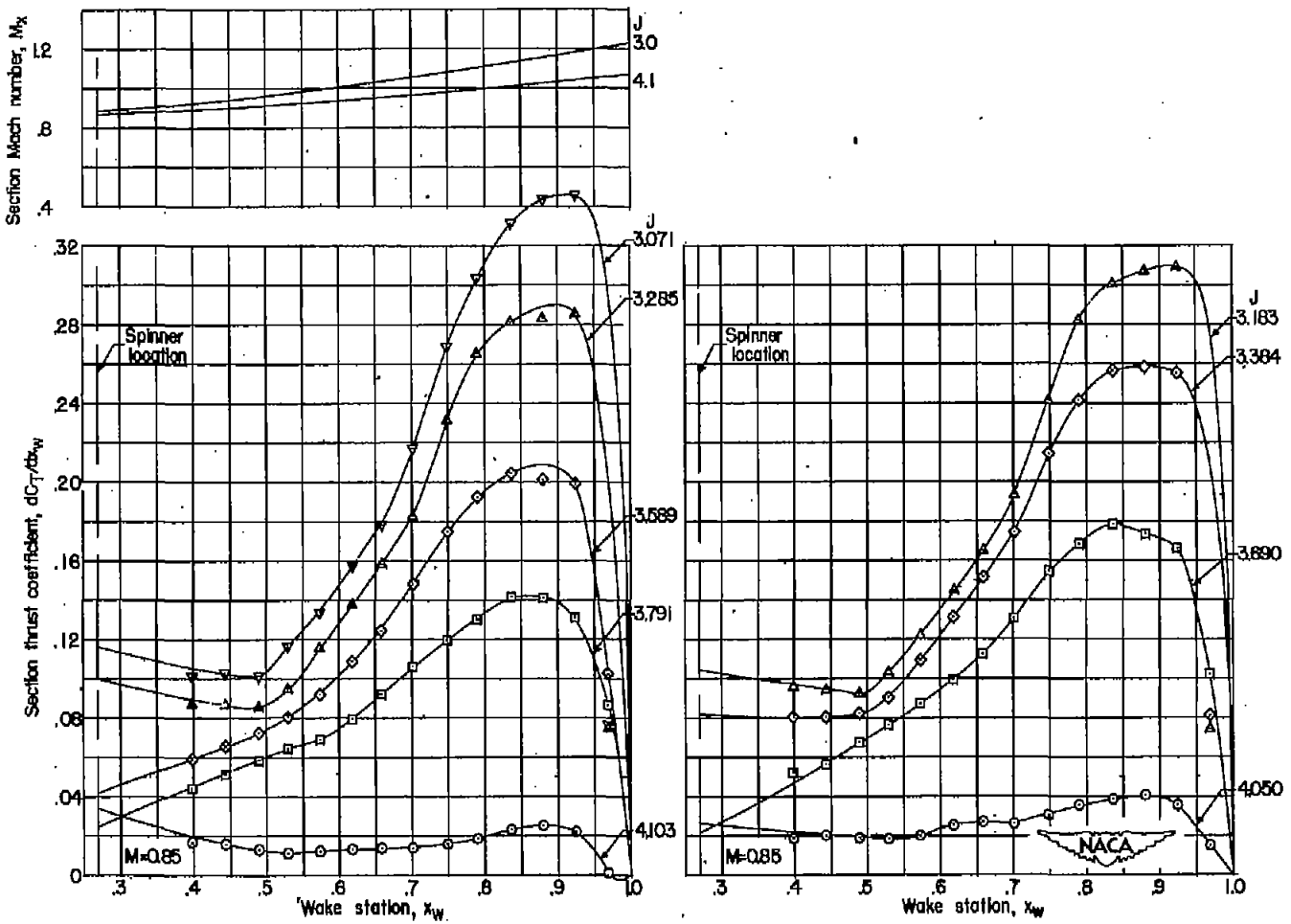

(d) Continued. $\beta_{0.75R} = 60°$.

Figure 5.- Continued.

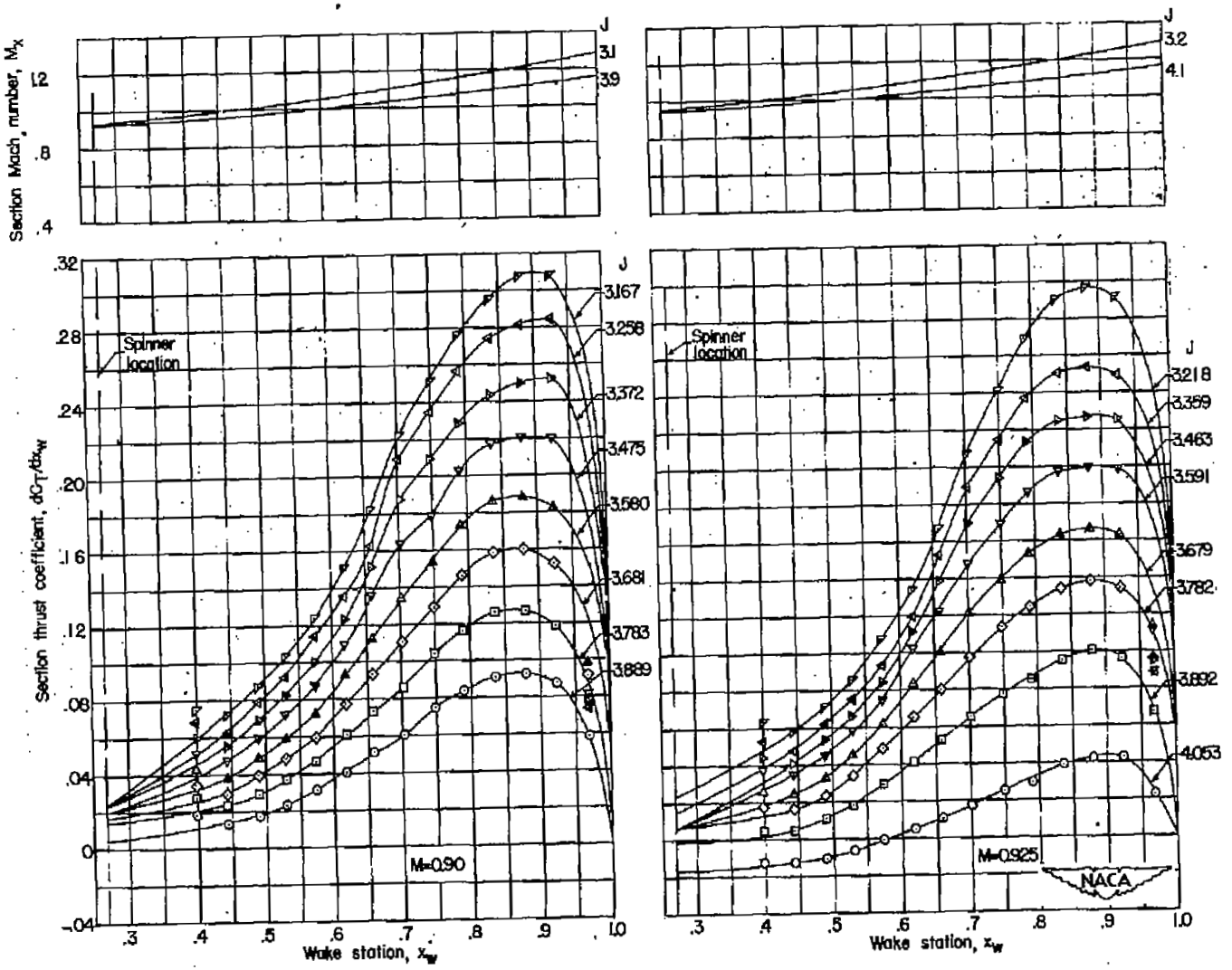

(d) Concluded. $\beta_{0.75R} = 60^\circ$.

Figure 5.- Continued.

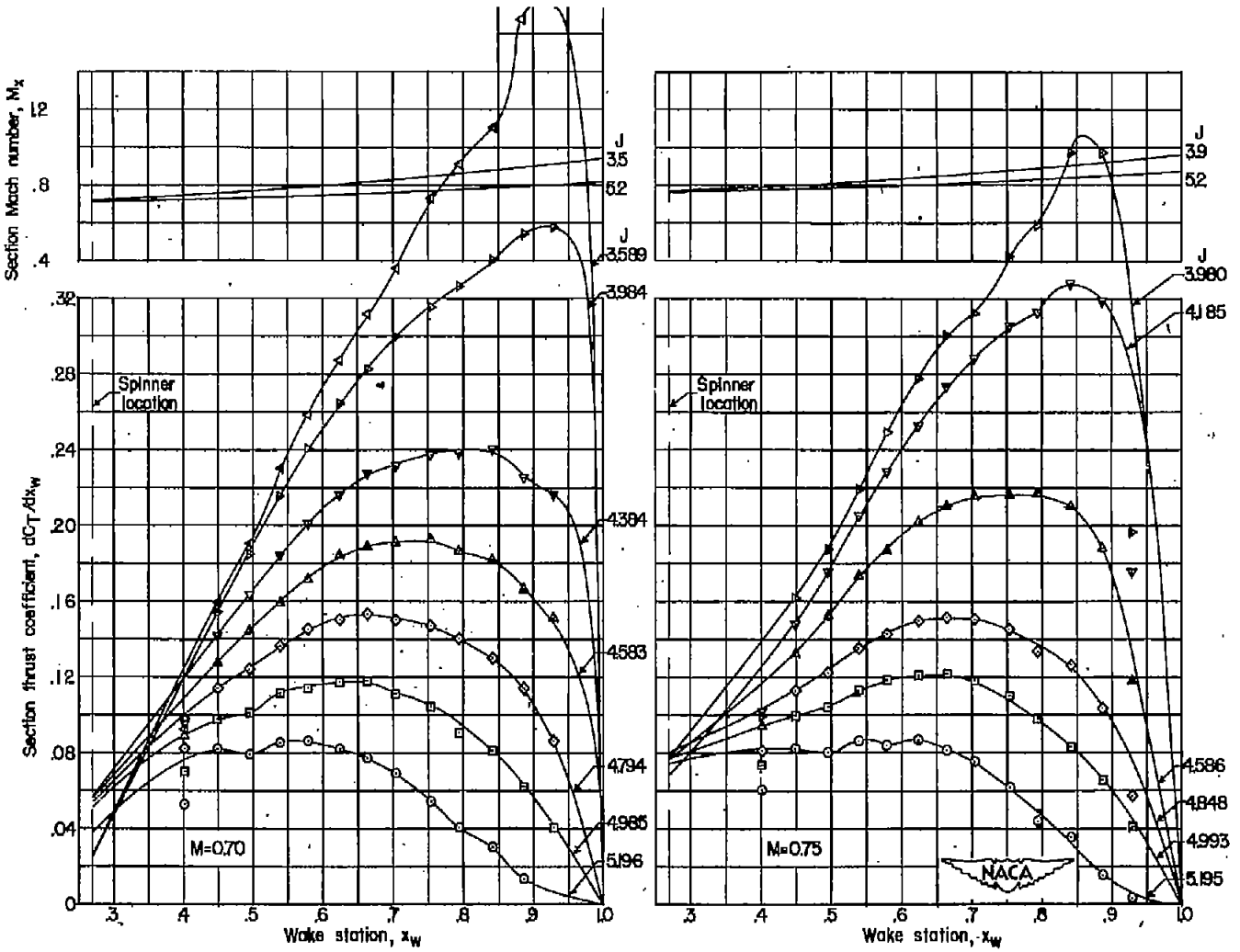

(e) $\beta_{0.75R} = 65^\circ$.

Figure 5.- Continued.

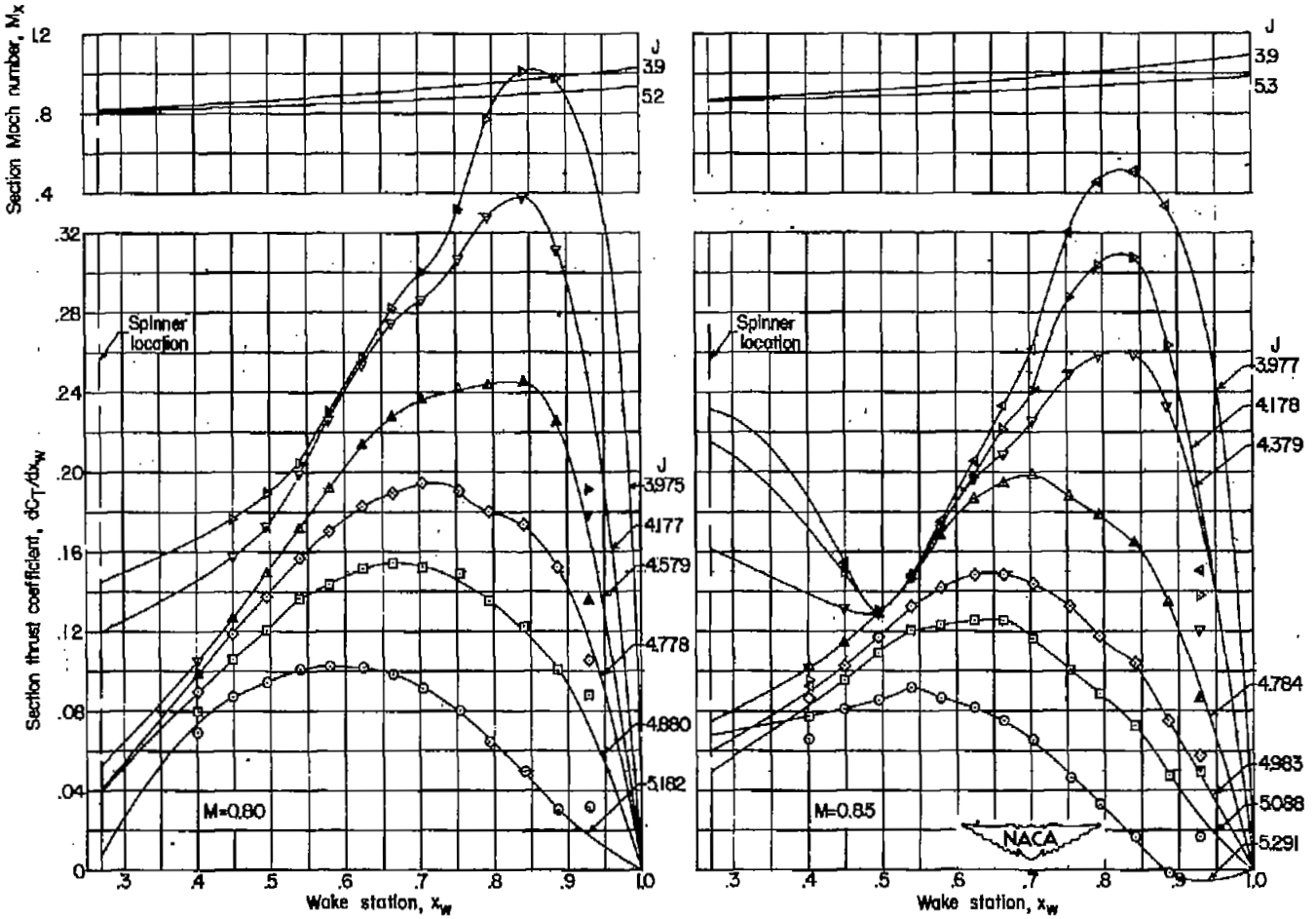

(e) Continued. $\beta_{0.75R} = 65°$.

Figure 5.- Continued.

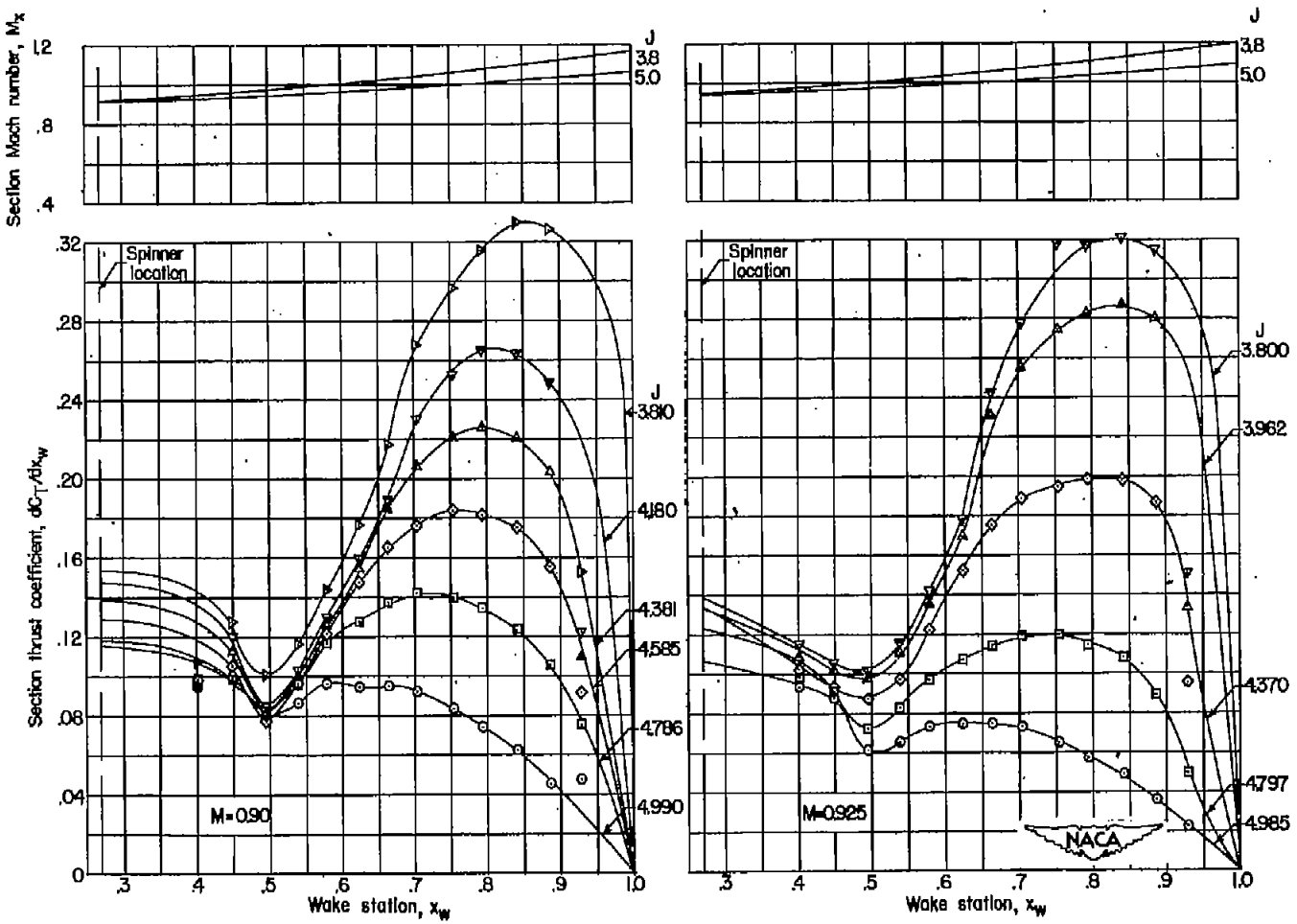

(e) Concluded. $\beta_{0.75R} = 65°$.

Figure 5.- Concluded.

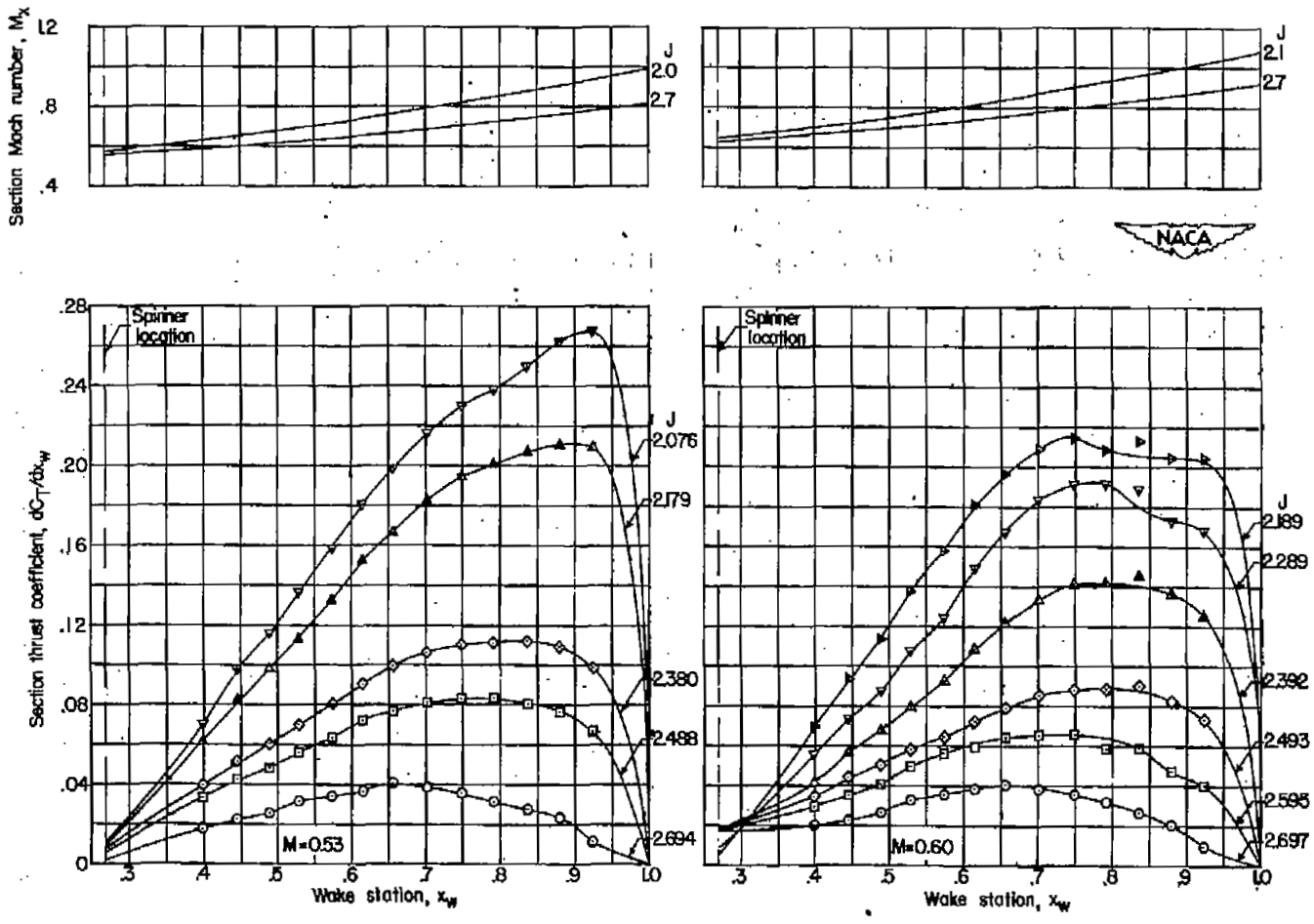

(a) $\beta_{0.75R} = 50^\circ$.

Figure 6.- Basic section-thrust-coefficient curves for NACA 4-(0)(08)-045 propeller.

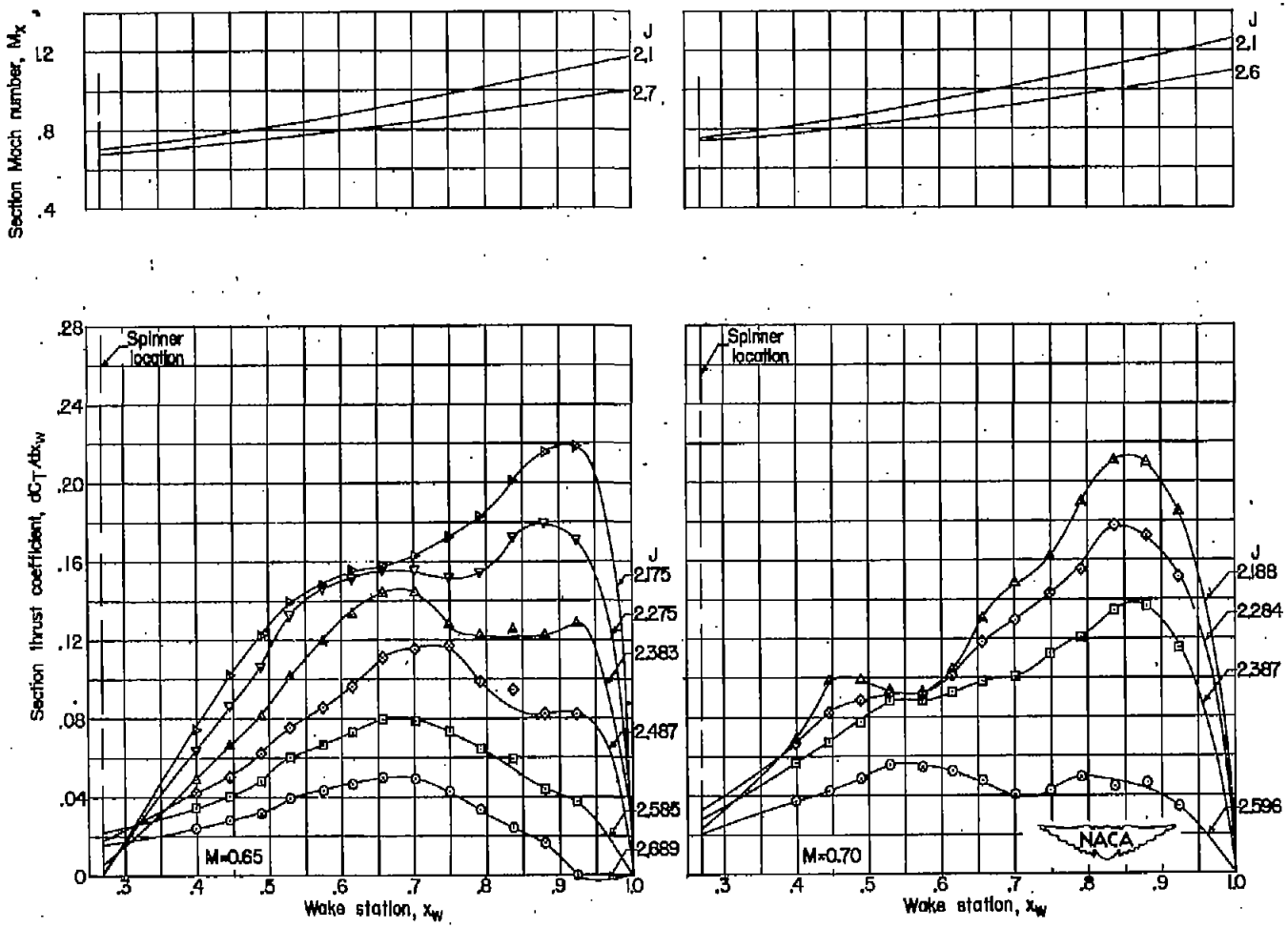

(a) Continued. $\beta_{0.75R} = 50^\circ$.

Figure 6.- Continued.

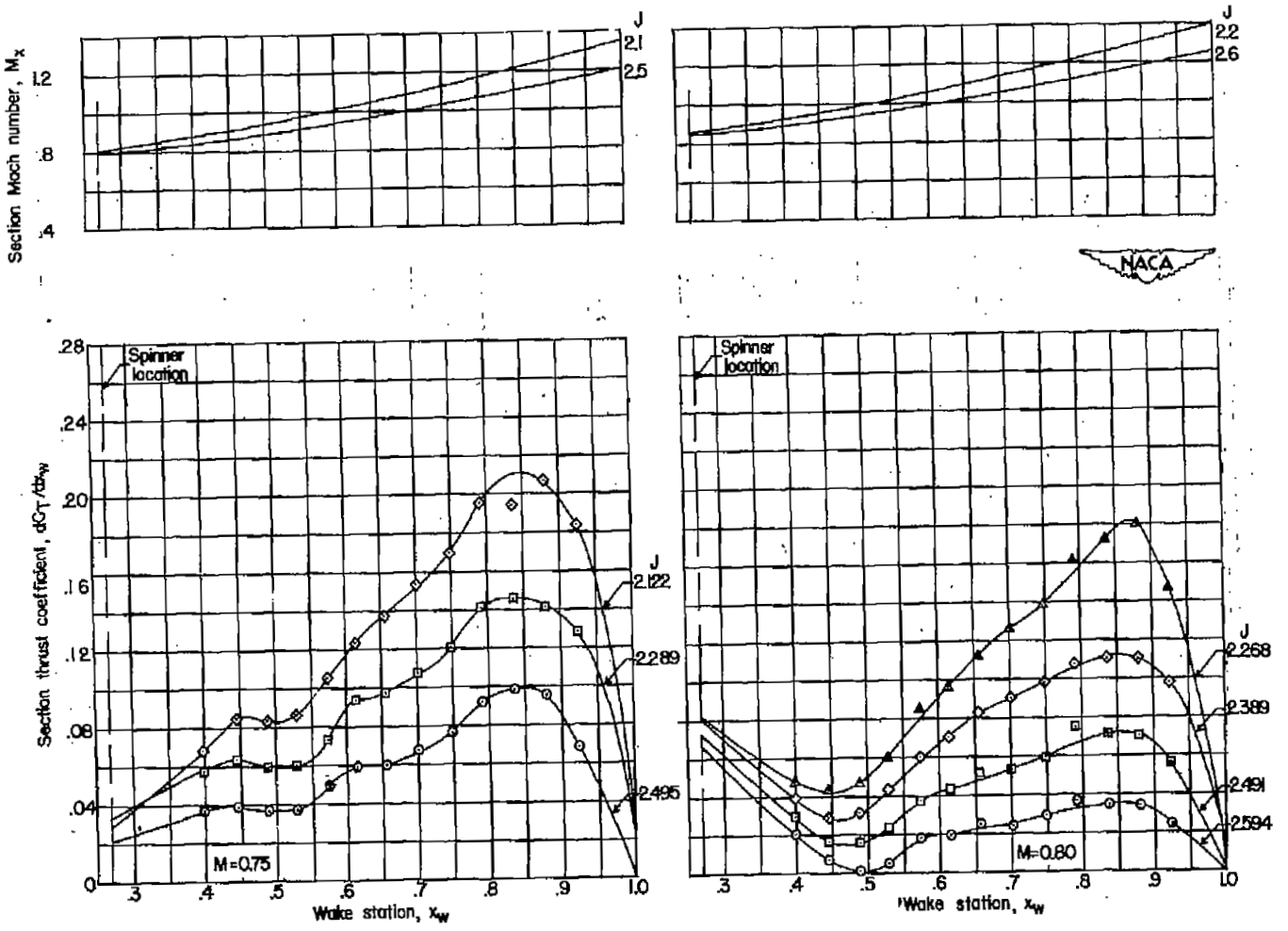

(a) Concluded. $\beta_{0.75R} = 50^\circ$.

Figure 6.- Continued.

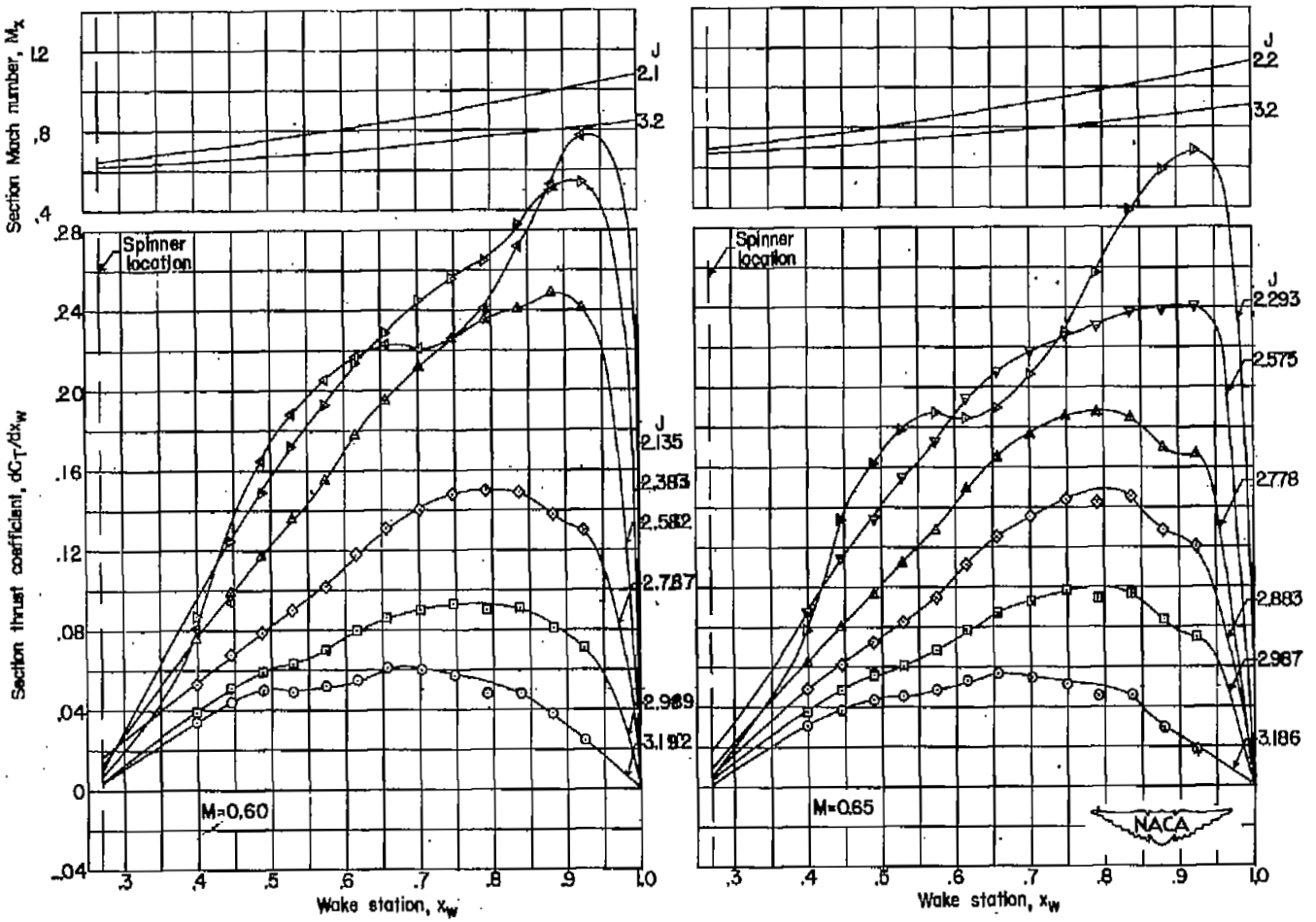

(b) $\beta_{0.75R} = 55°$.

Figure 6.- Continued.

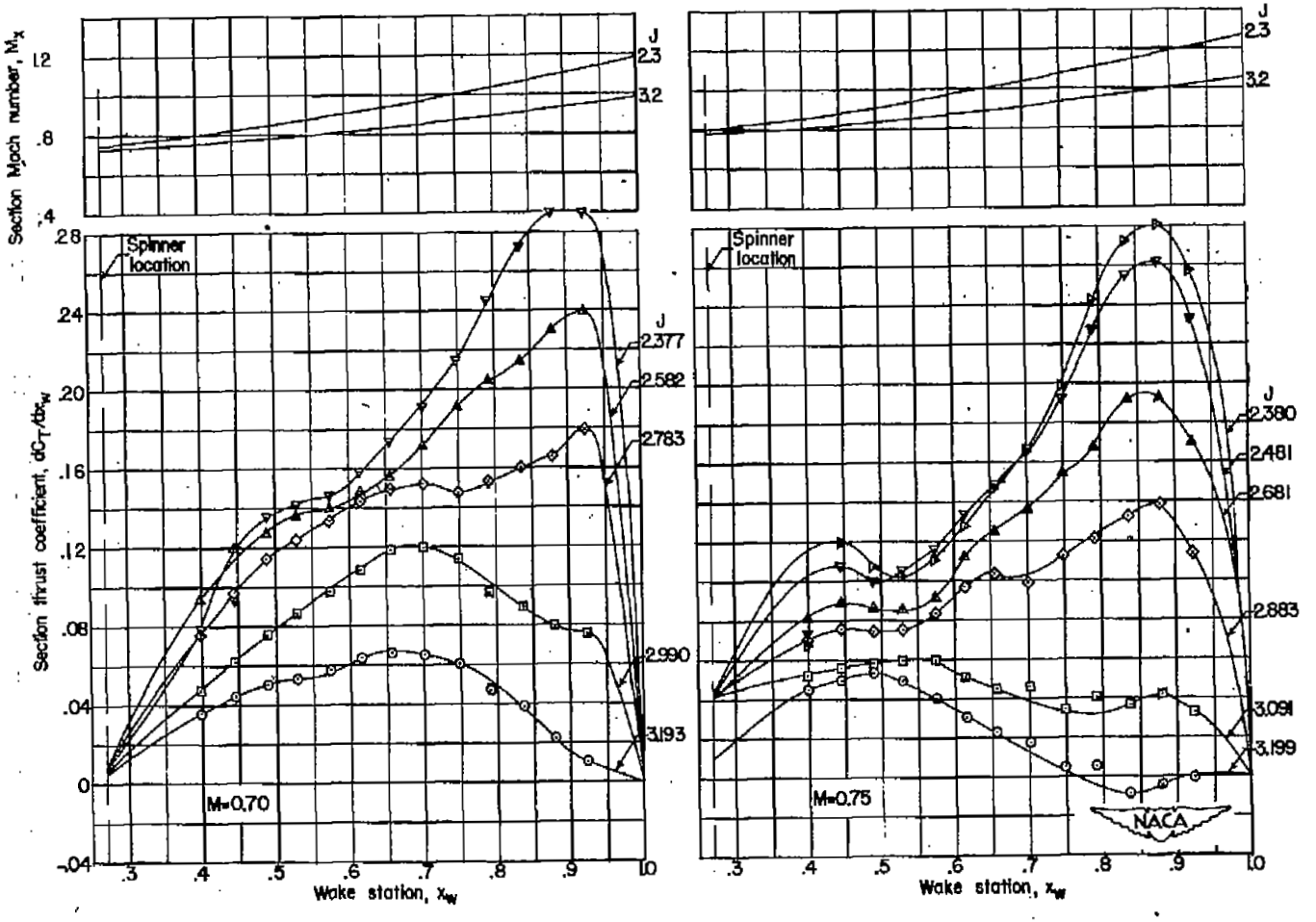

(b) Continued. $\beta_{0.75R} = 55°$.

Figure 6.- Continued.

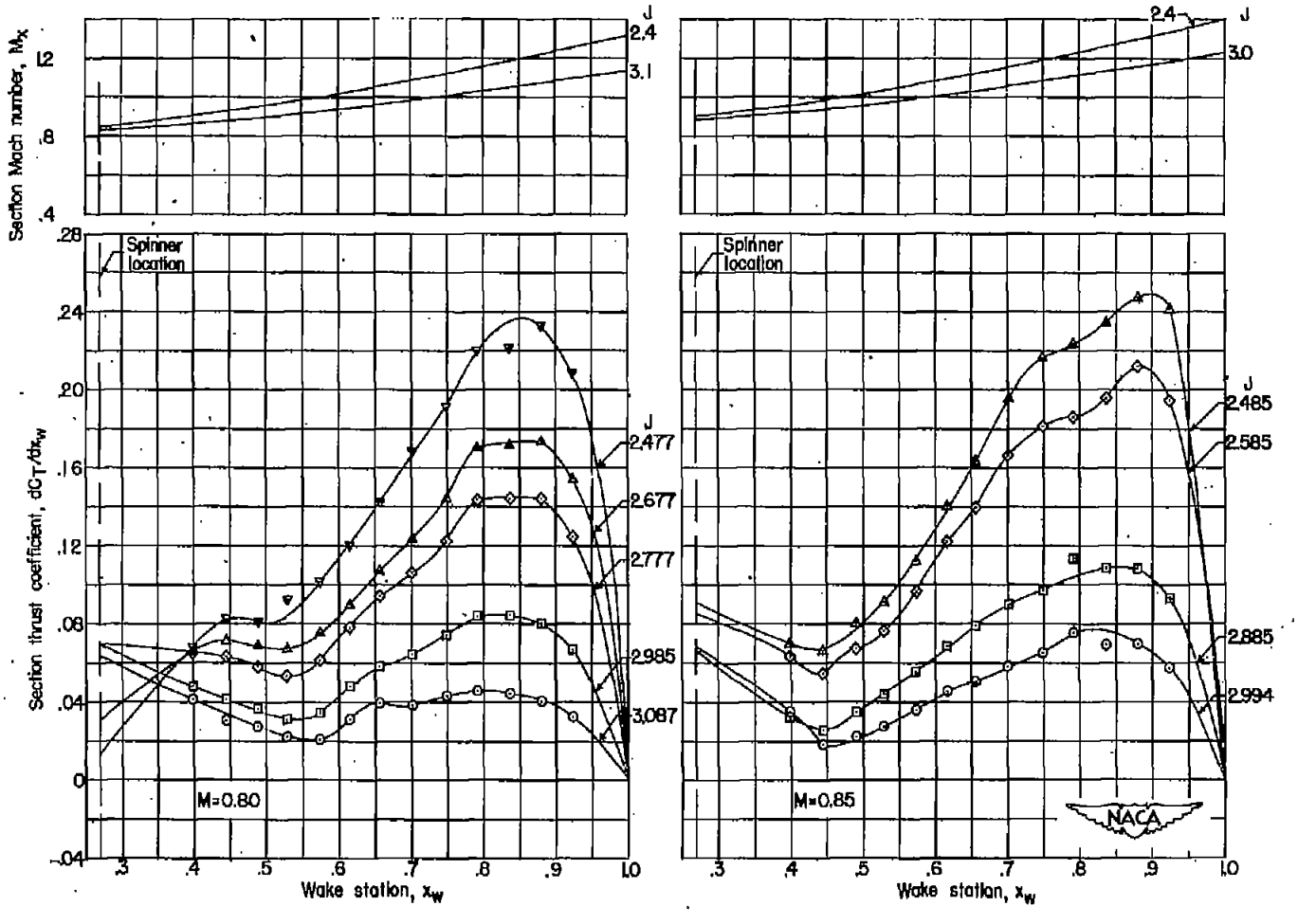

(b) Continued. $\beta_{0.75R} = 55^\circ$.

Figure 6.- Continued.

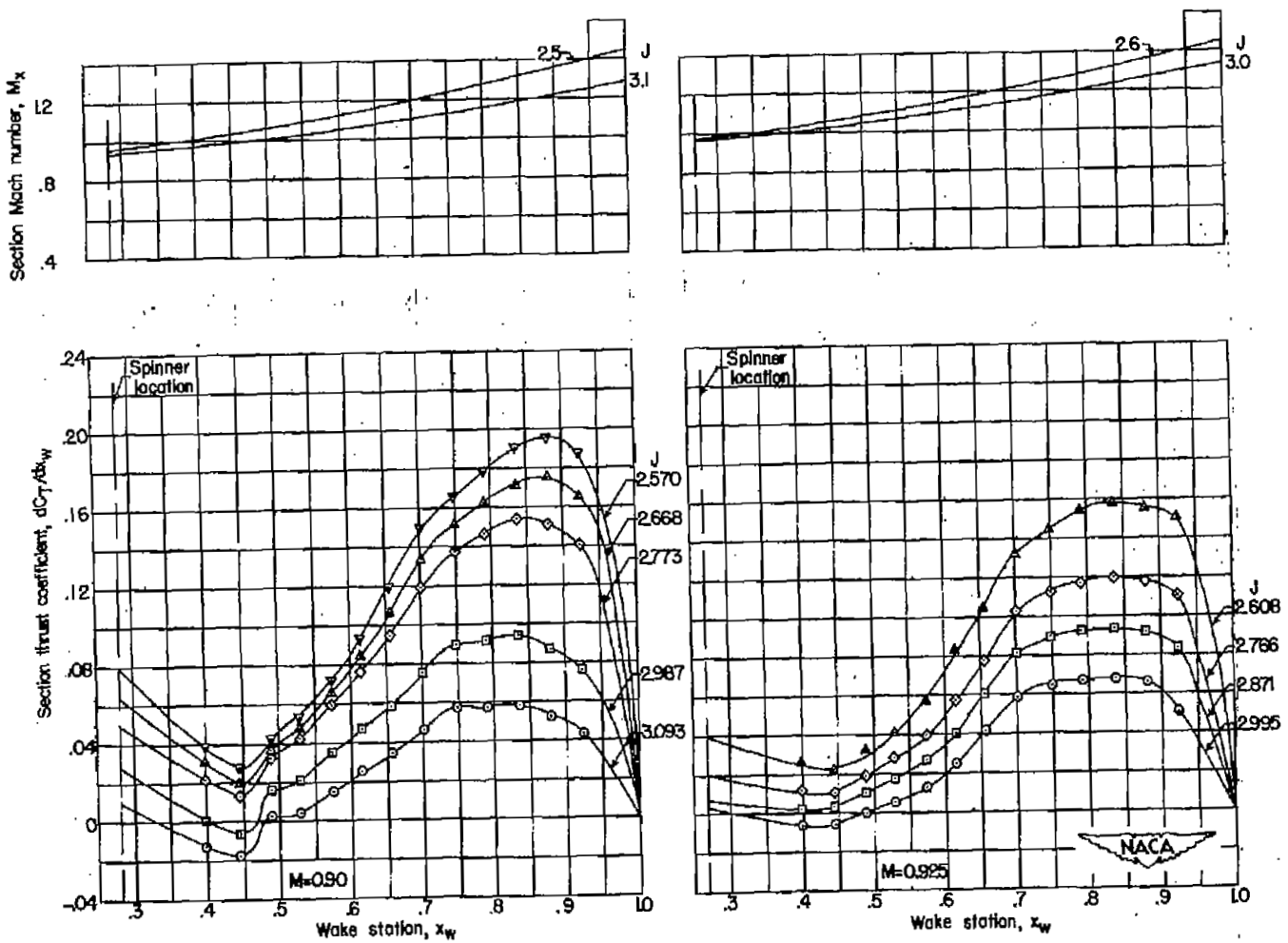

(b) Concluded. $\beta_{0.75R} = 55^{\circ}$.

Figure 6.- Continued.

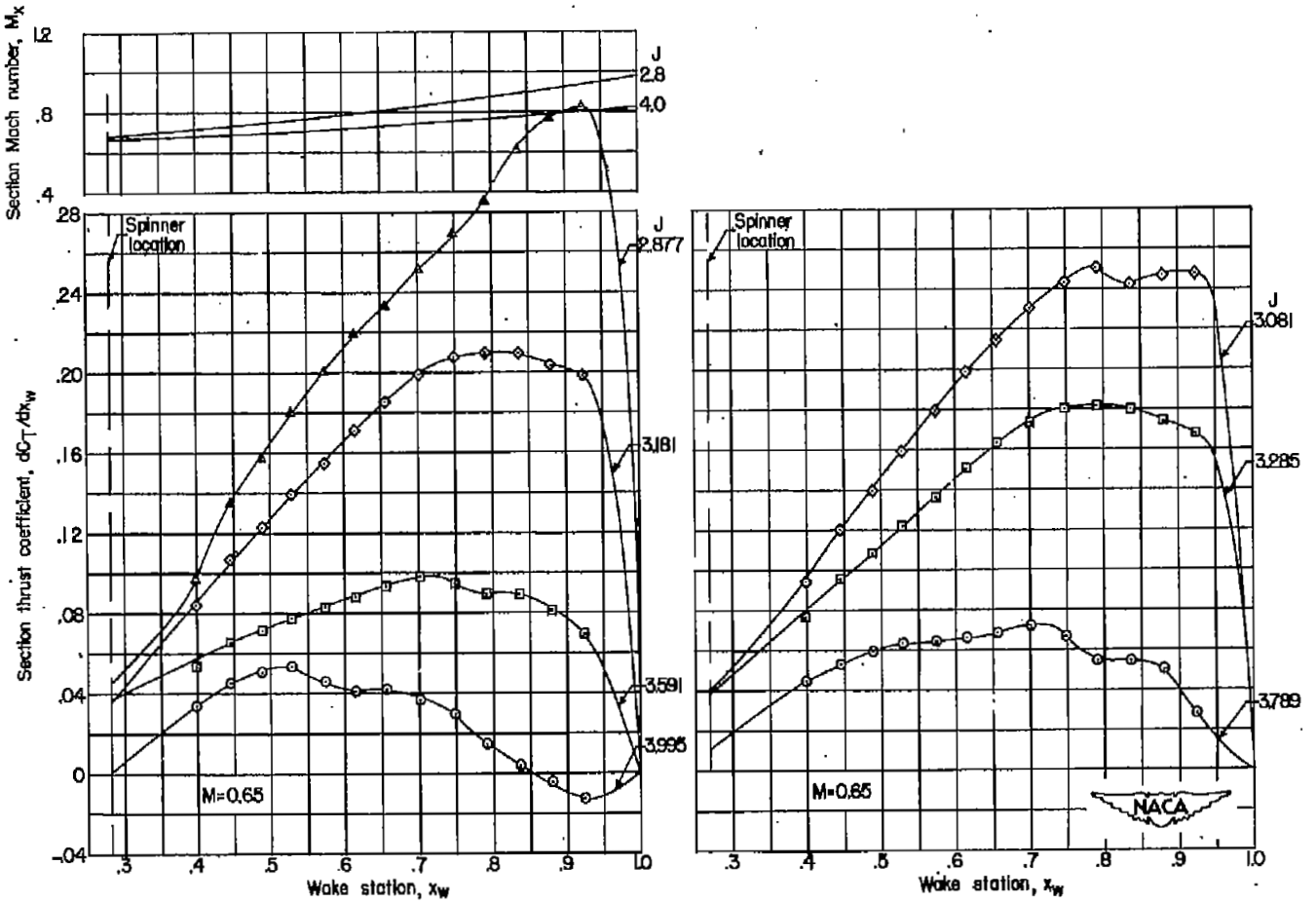

(c) $\beta_{0.75R} = 60°$.

Figure 6.- Continued.

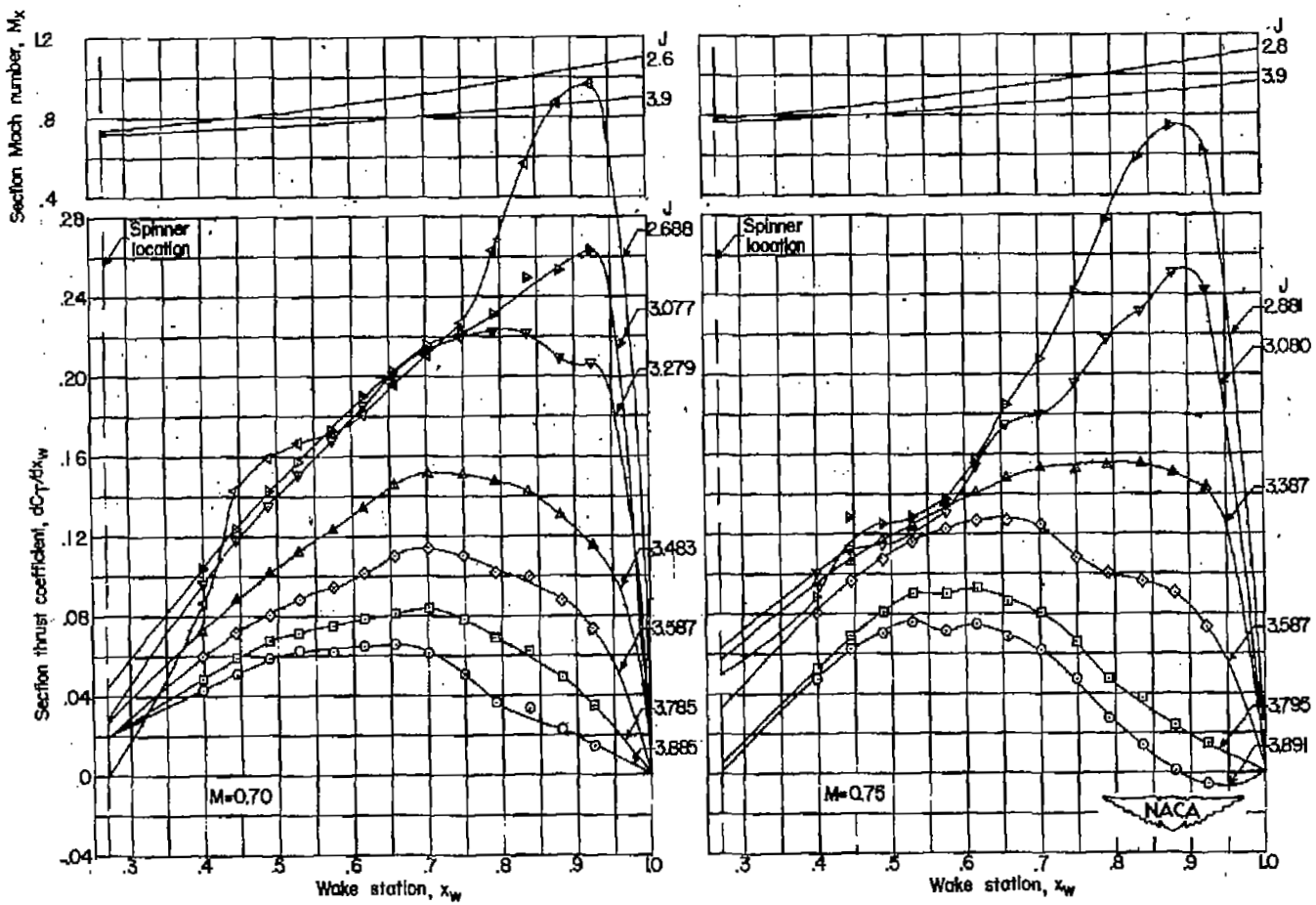

(c) Continued. $\beta_{0.75R} = 60^\circ$.

Figure 6.- Continued.

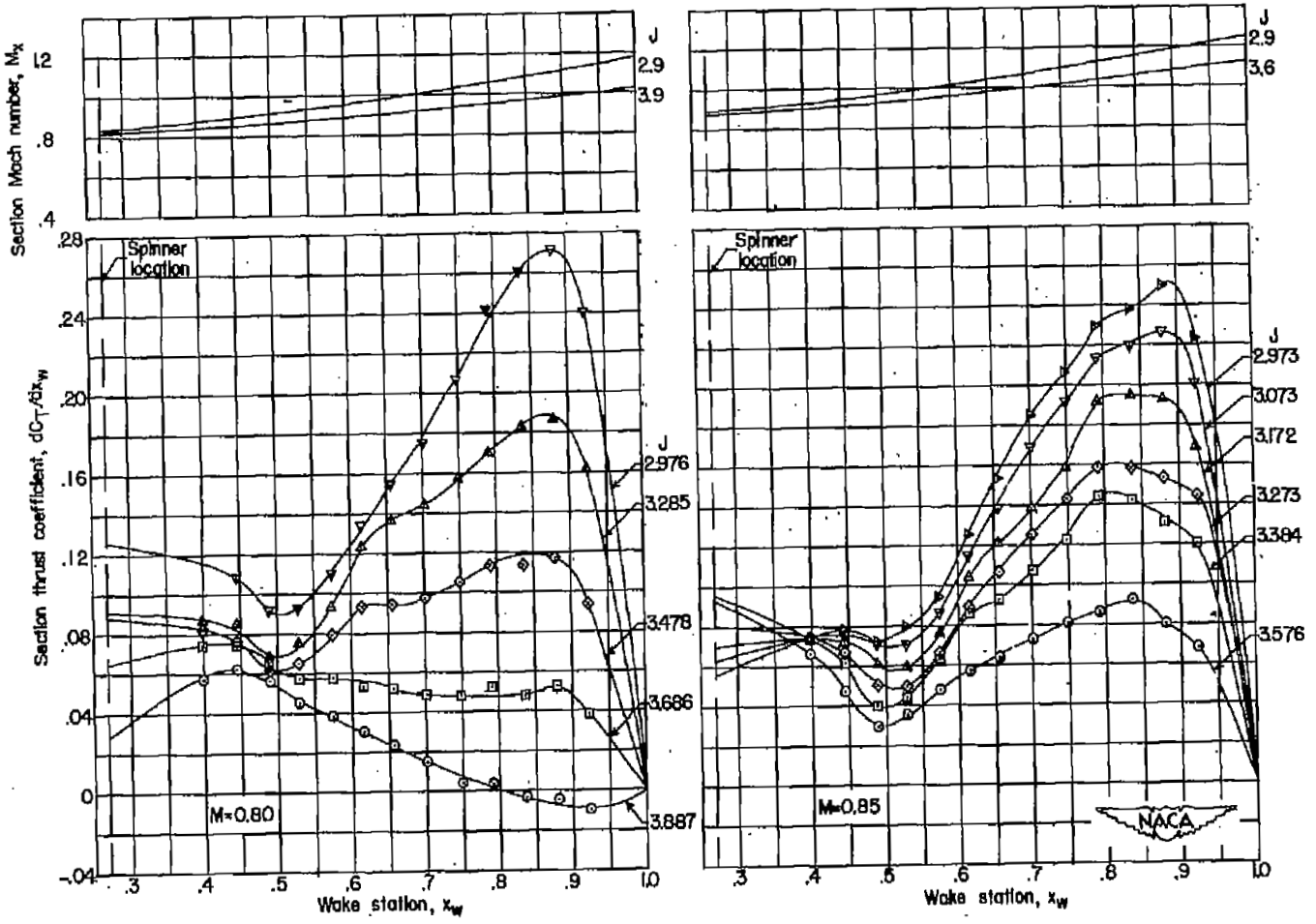

(c) Continued. $\beta_{0.75R} = 60°$.

Figure 6.- Continued.

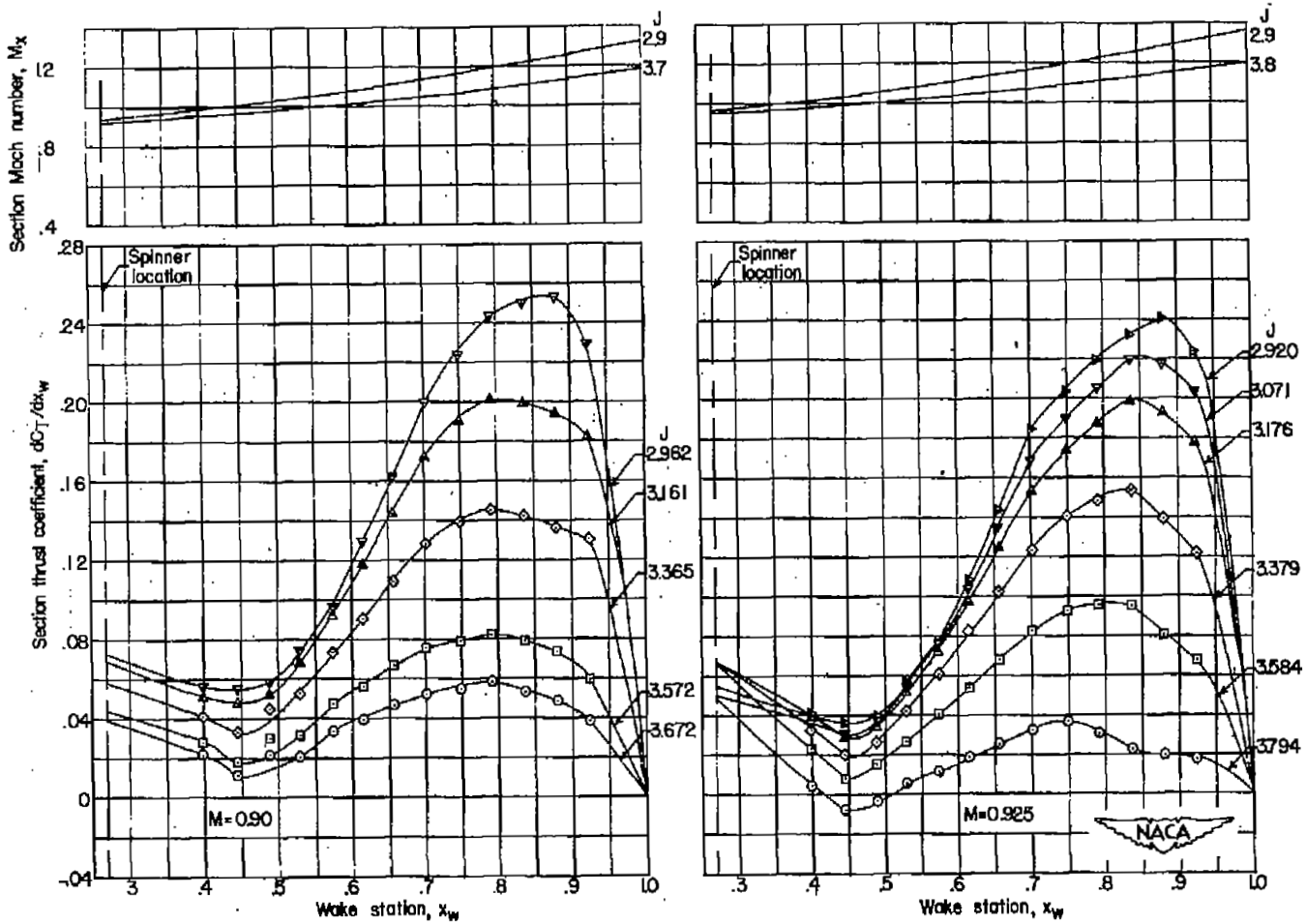

(c) Concluded. $\beta_{0.75R} = 60°$.

Figure 6.- Continued.

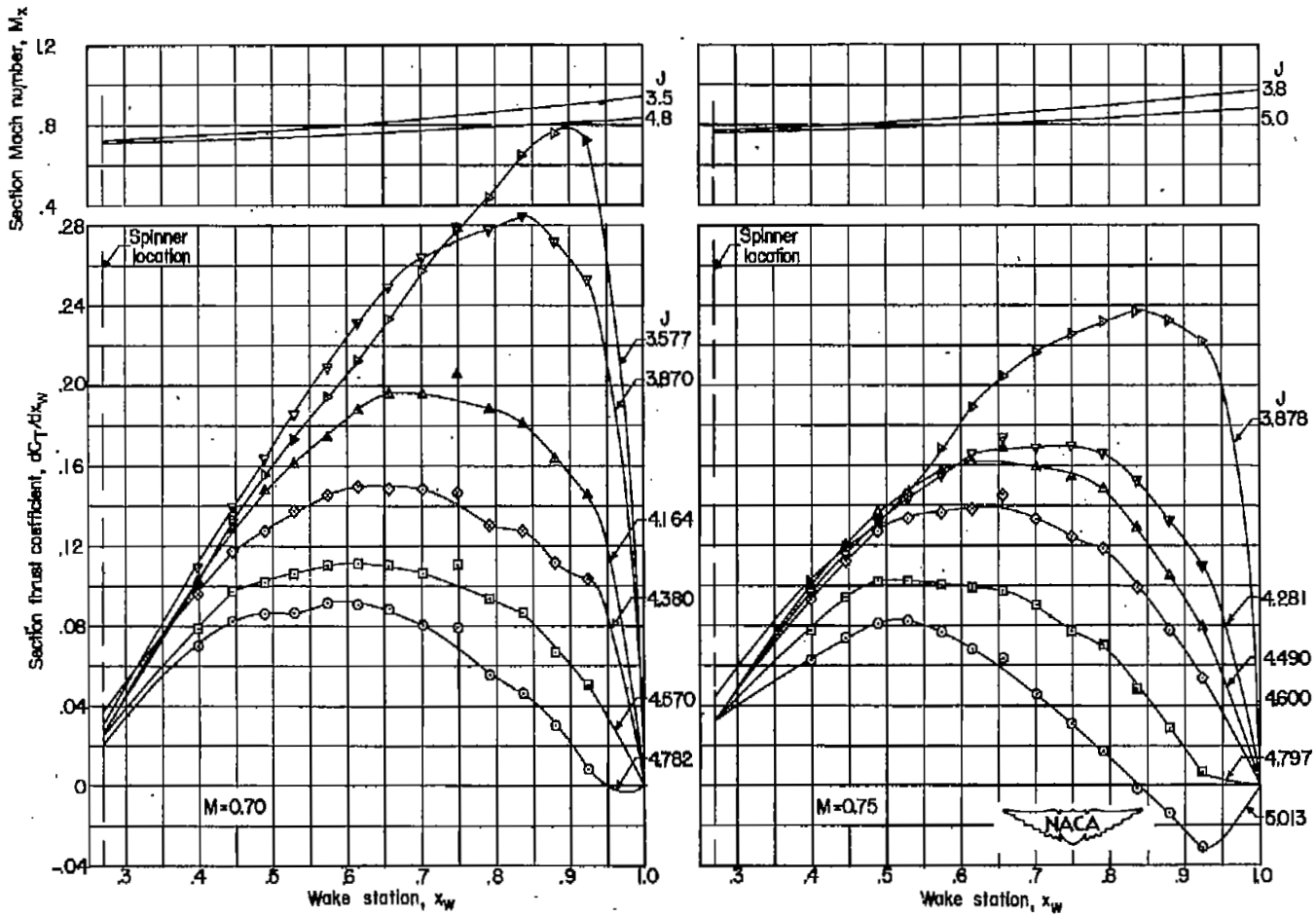

(d) $\beta_{0.75R} = 65°$.

Figure 6.- Continued.

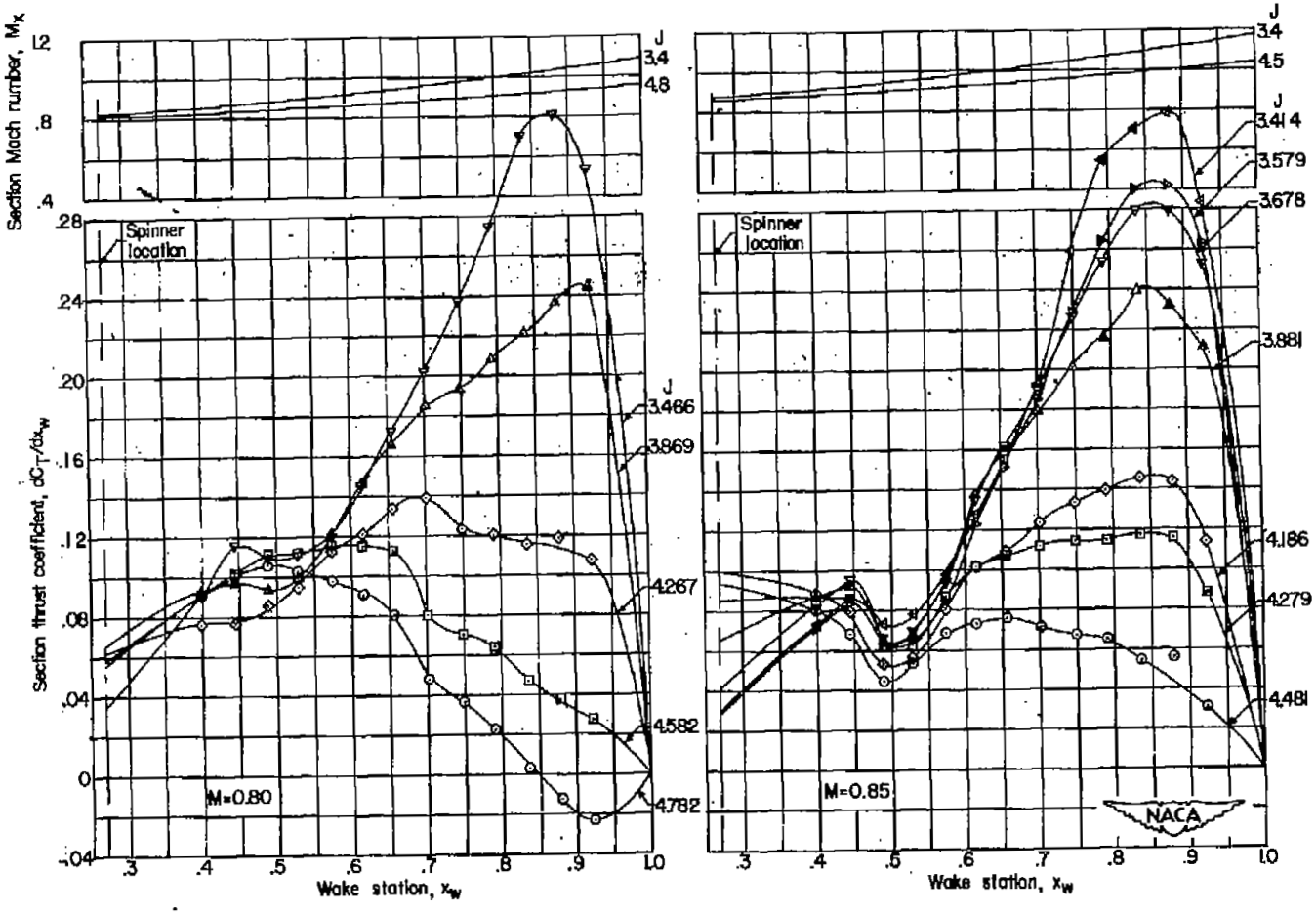

(d) Continued. $\beta_{0.75R} = 65°$.

Figure 6.- Continued.

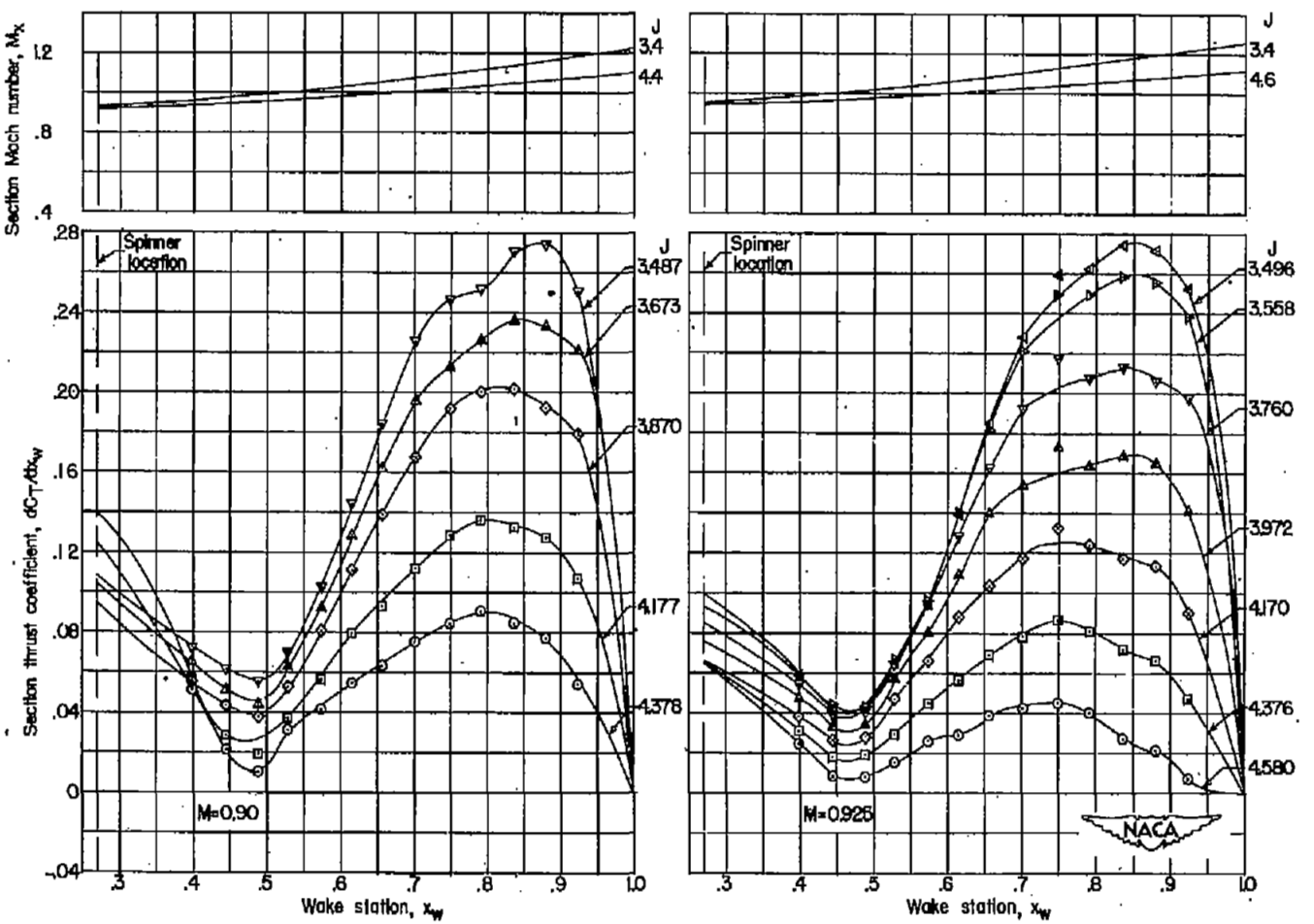

(d) Concluded. $\beta_{0.75R} = 65°$.

Figure 6.- Concluded.

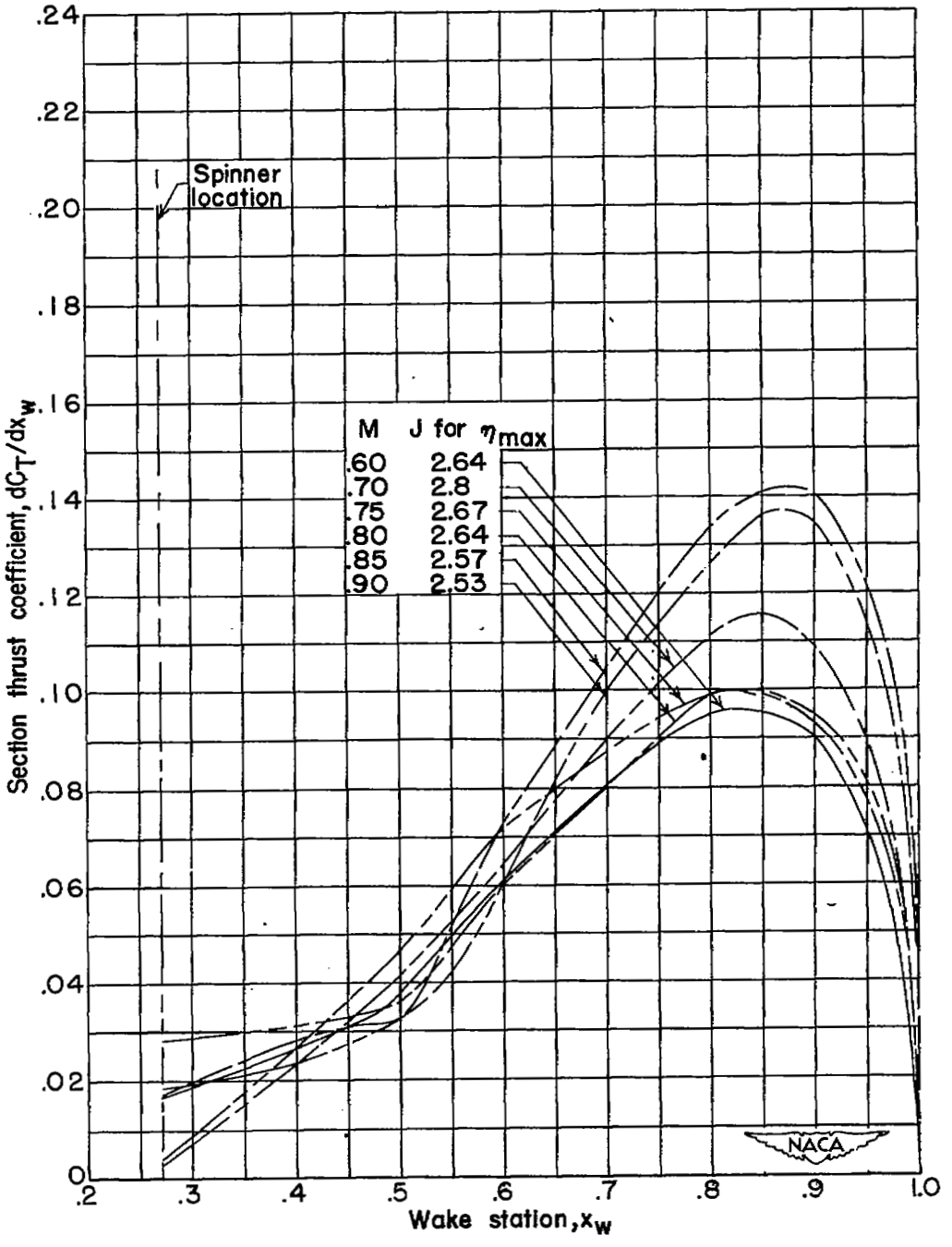

(a) $\beta_{0.75R} = 50^\circ$.

Figure 7.- Effect of forward Mach number on section-thrust-coefficient curves for maximum efficiency. NACA 4-(0)(03)-045 propeller.

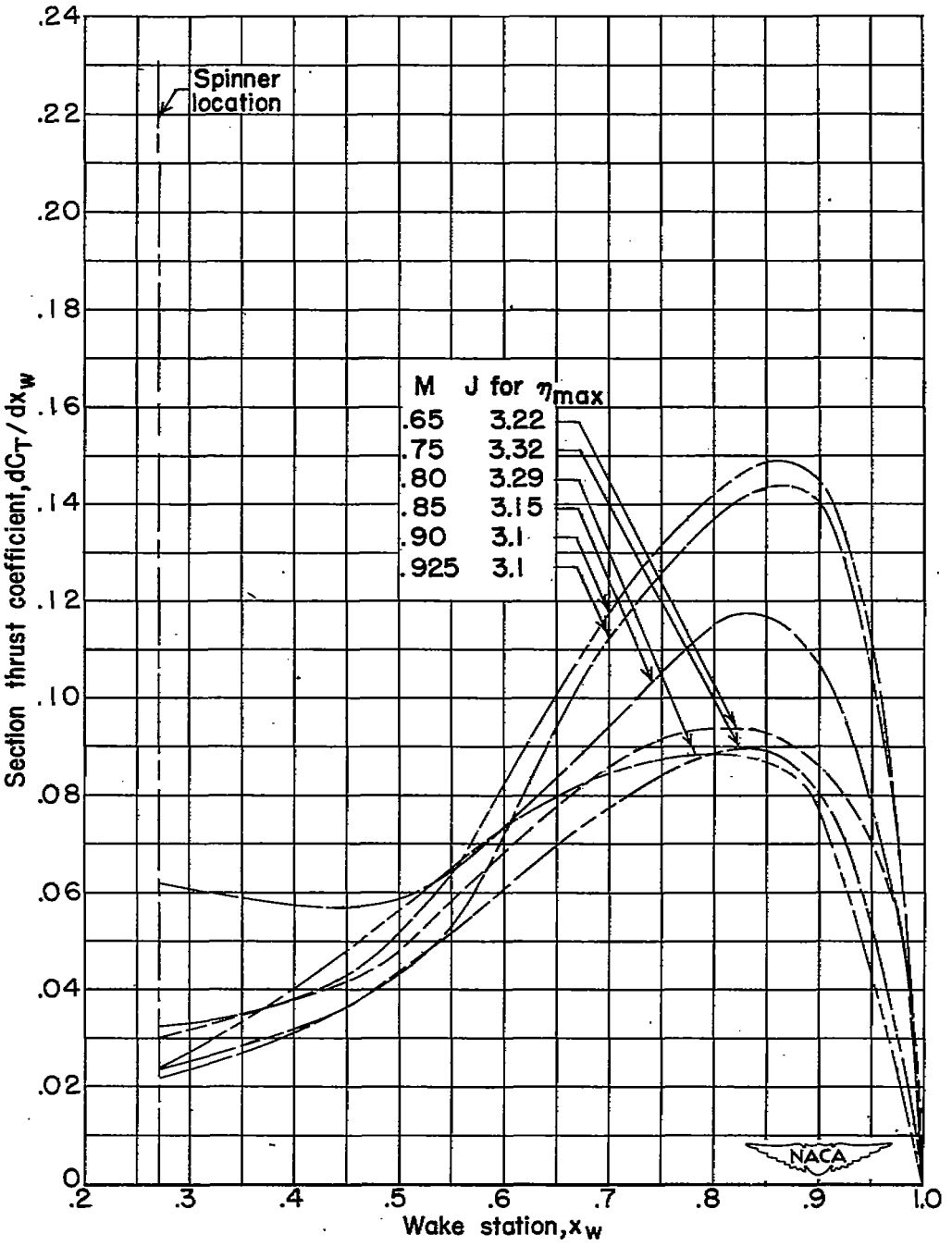

(b) $\beta_{0.75R} = 55^{\circ}$.

Figure 7.- Continued.

[redacted]

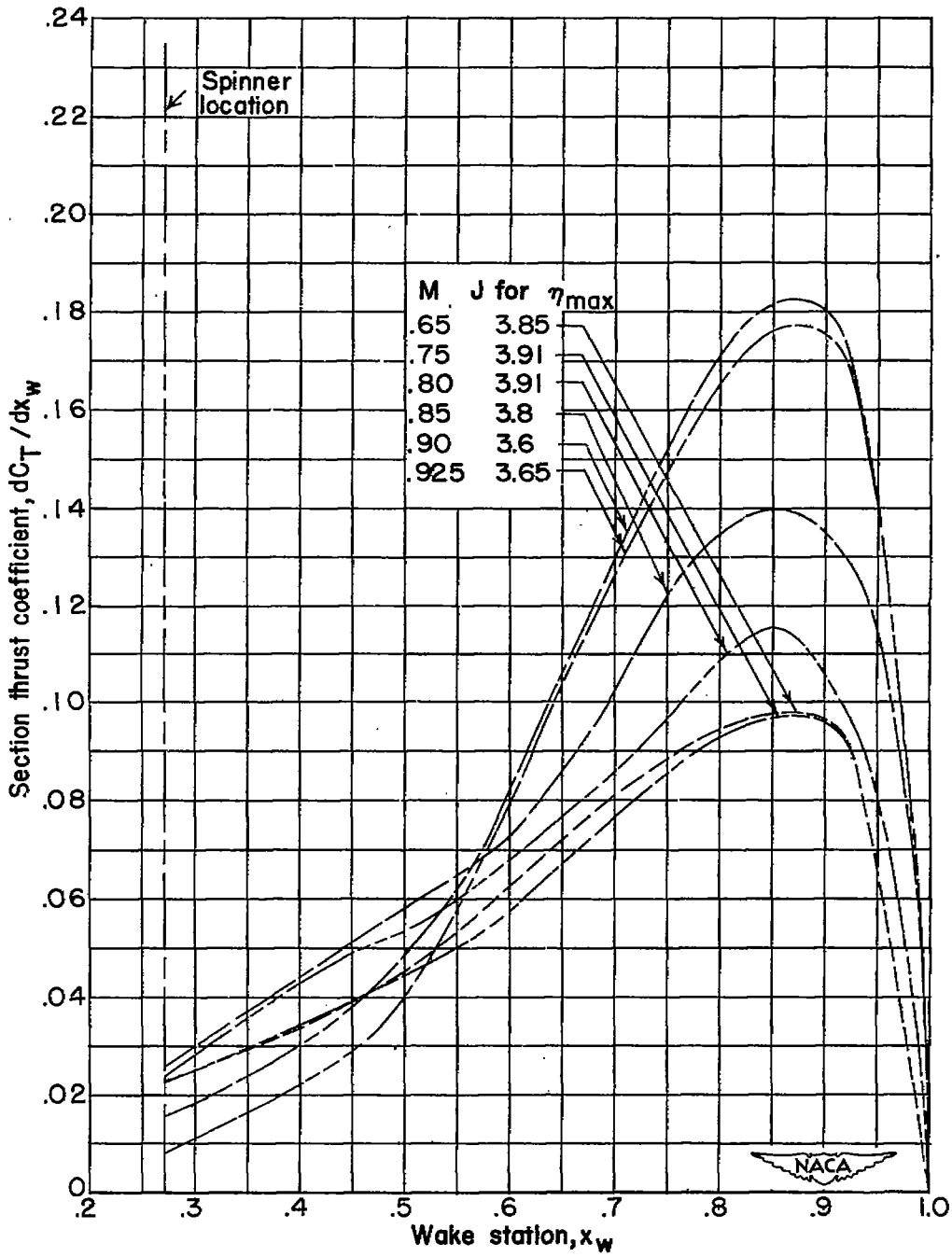

(c) $\beta_{0.75R} = 60^{\circ}$.

Figure 7.- Continued.

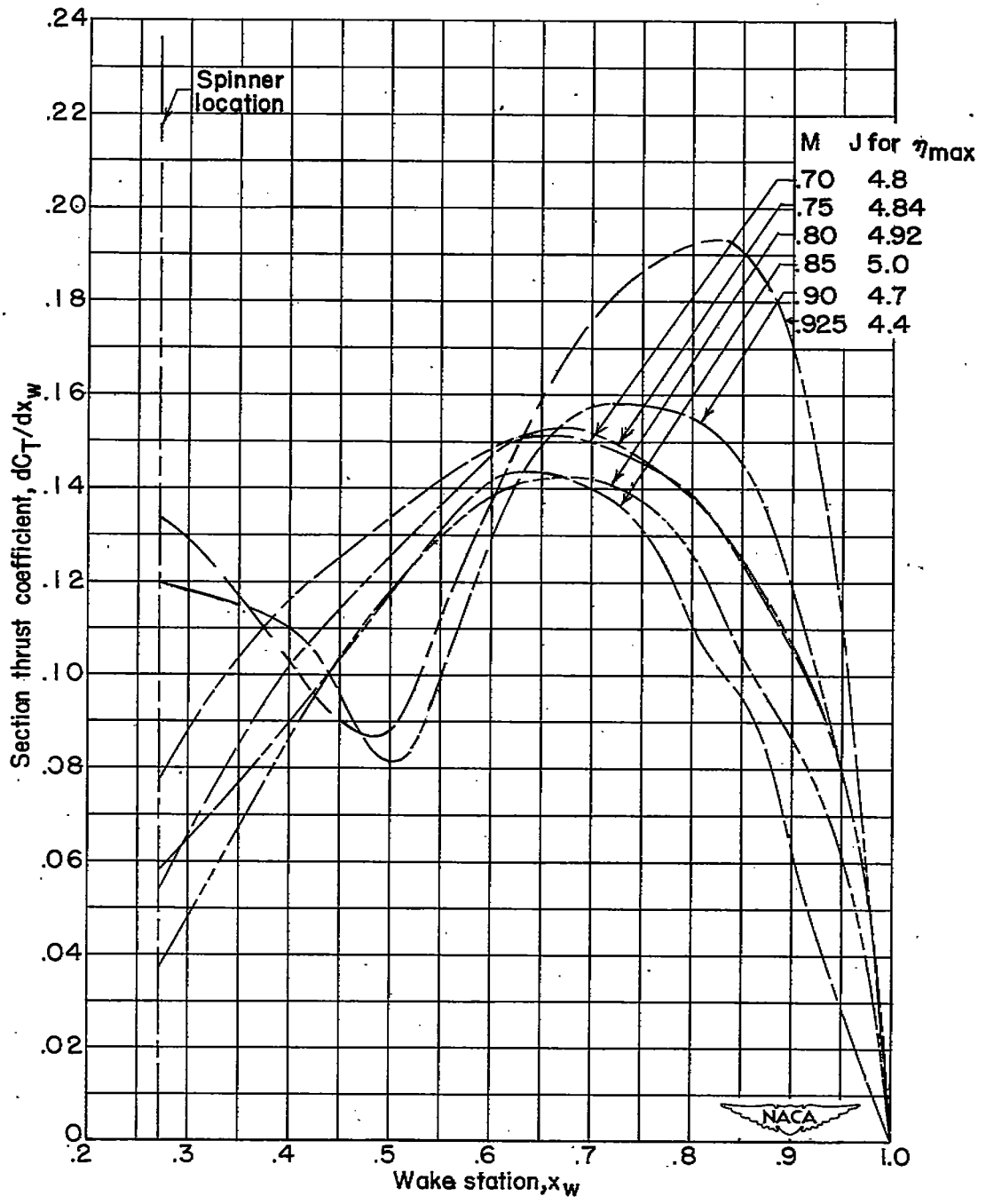

(d) $\beta_{0.75R} = 65°$.

Figure 7.- Concluded.

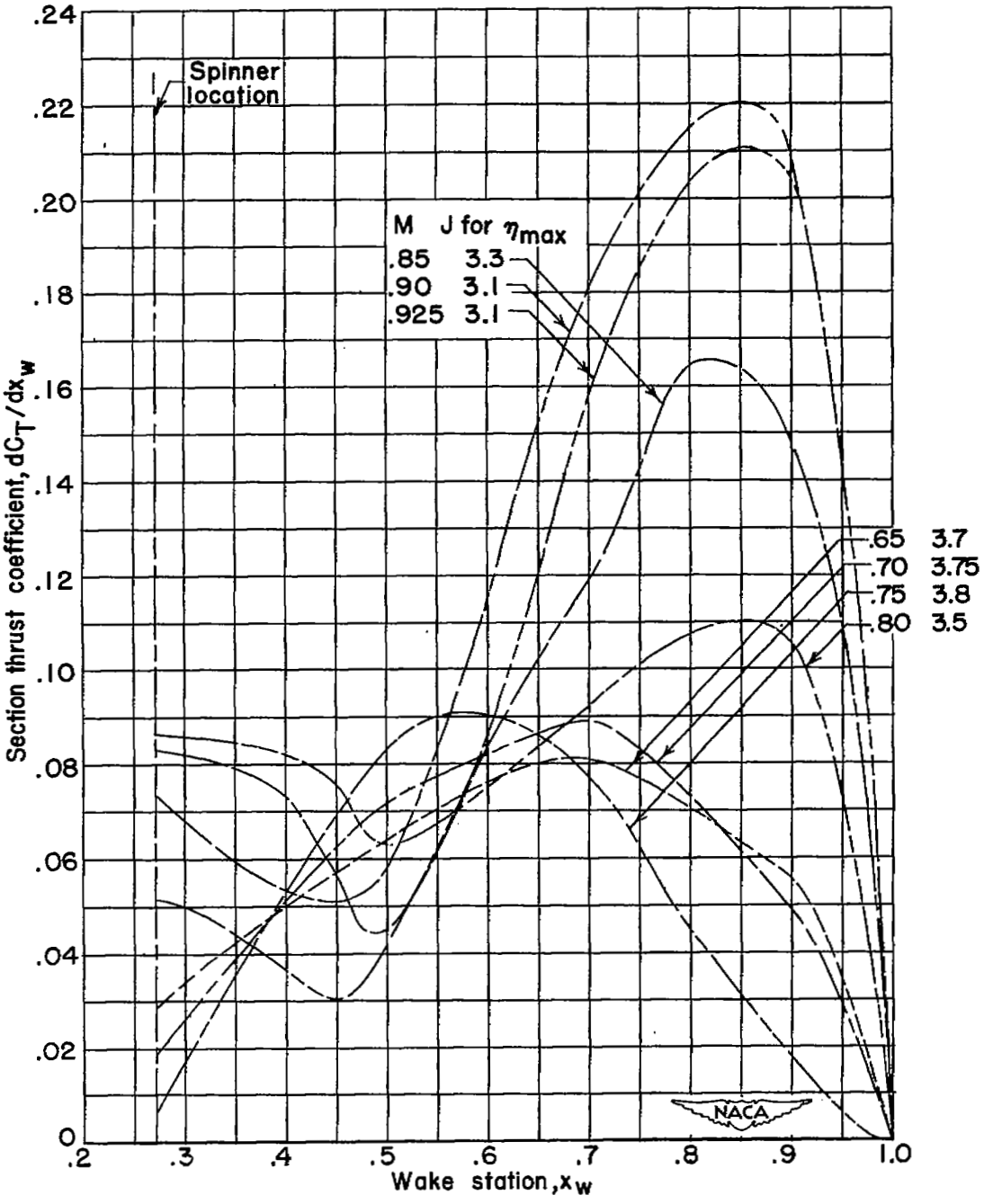

Figure 8.- Effect of forward Mach number on section-thrust-coefficient curves for maximum efficiency. NACA 4-(0)(08)-045 propeller. $\beta_{0.75R} = 60°$.

[redacted]

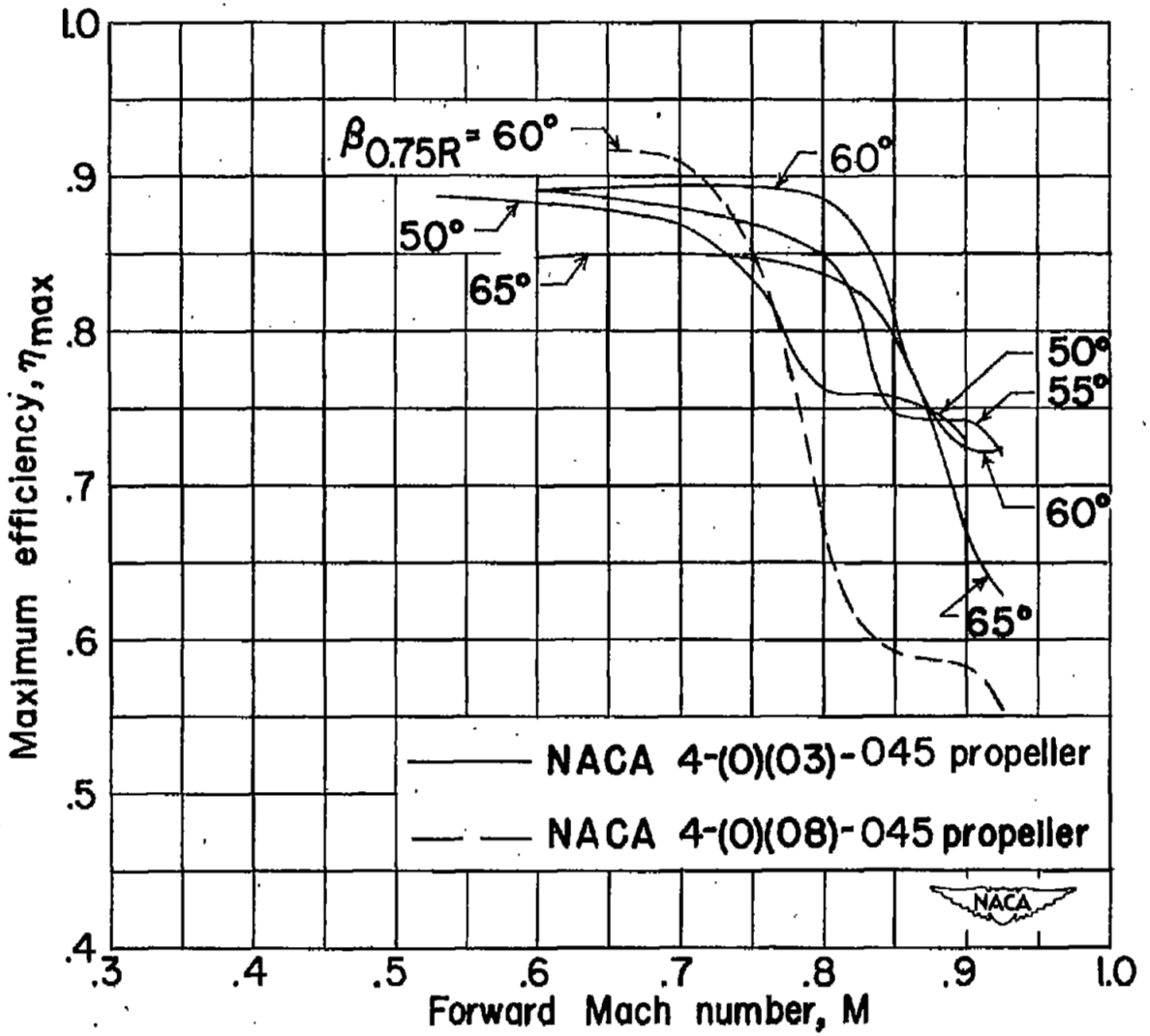

Figure 9.- Effect of forward Mach number on maximum efficiency.

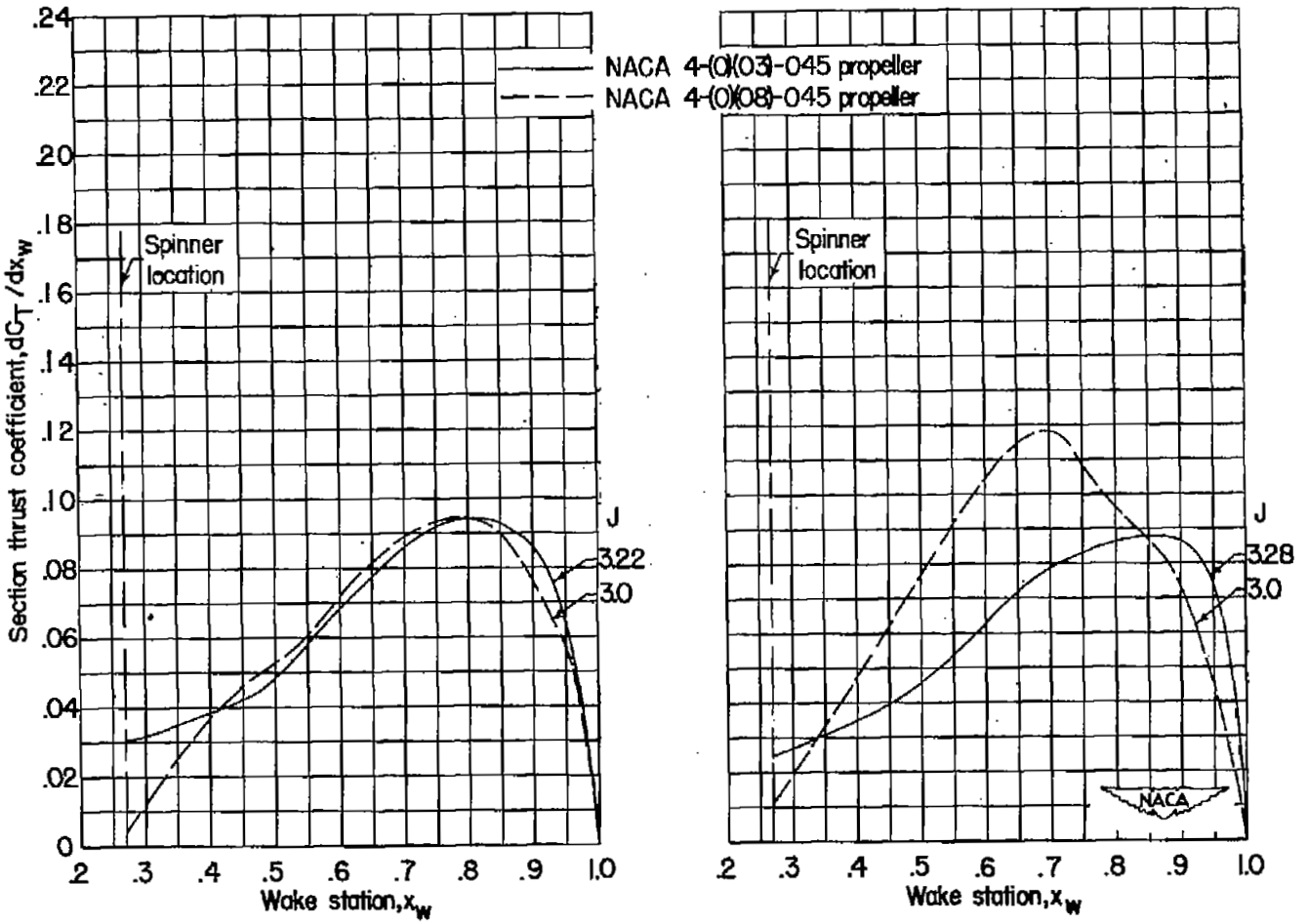

(a) M = 0.65. (b) M = 0.70.

Figure 10.- Effect of thickness ratio on section-thrust-coefficient curves at maximum efficiency. $\beta_{0.75R} = 55°$.

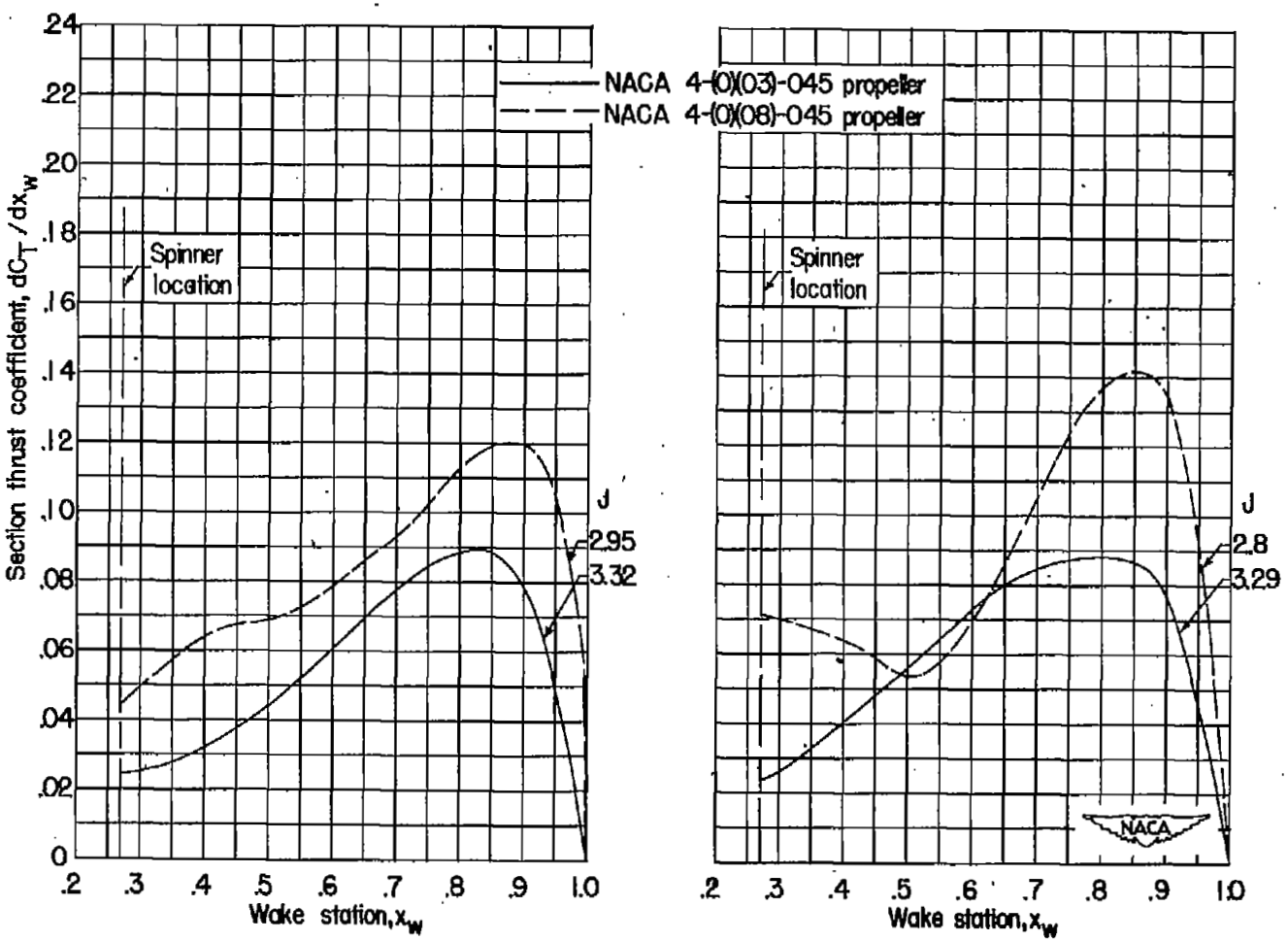

(c) M = 0.75.

(d) M = 0.80.

Figure 10.- Continued.

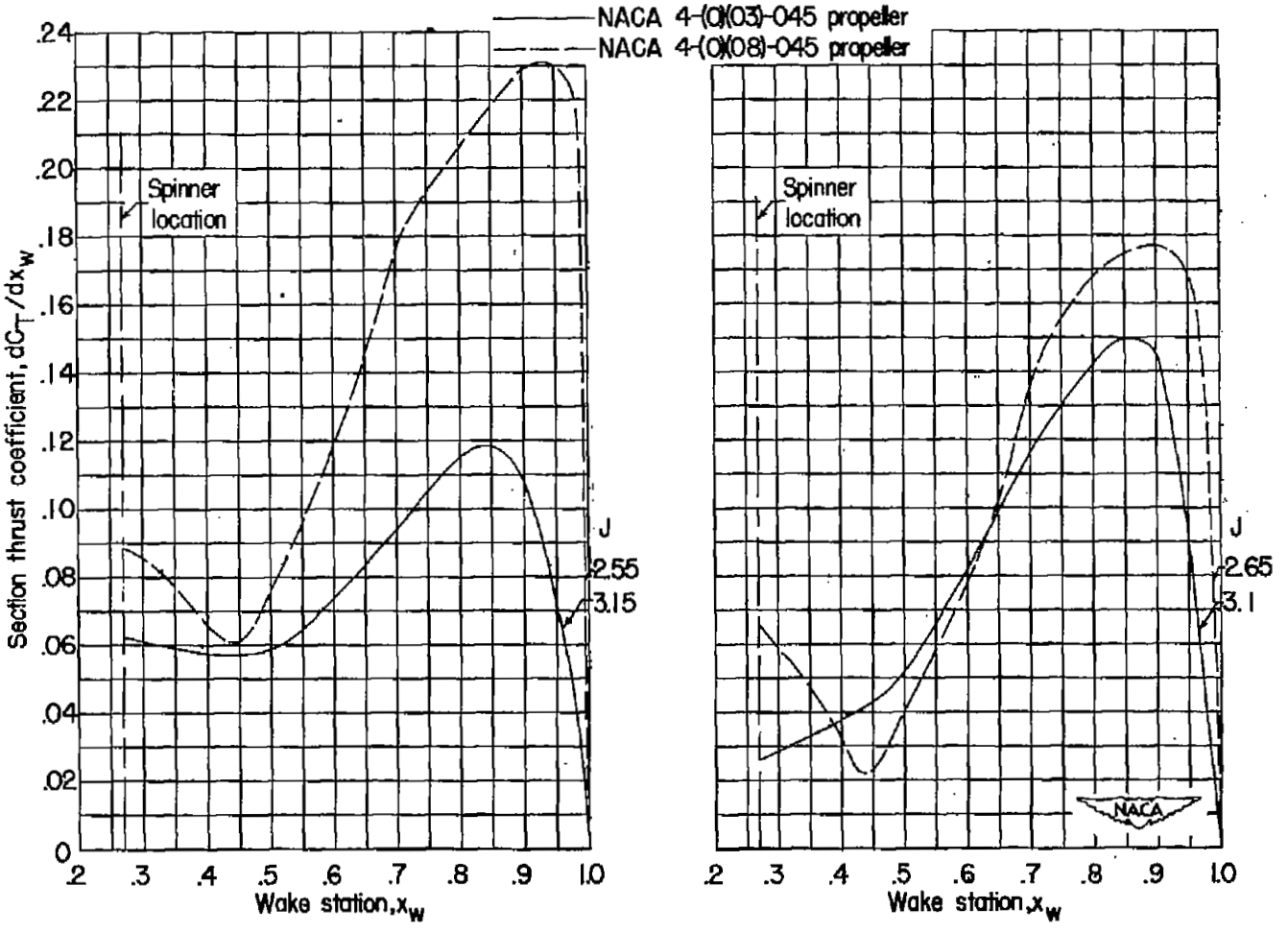

(e) M = 0.85.

(f) M = 0.90.

Figure 10.- Concluded.

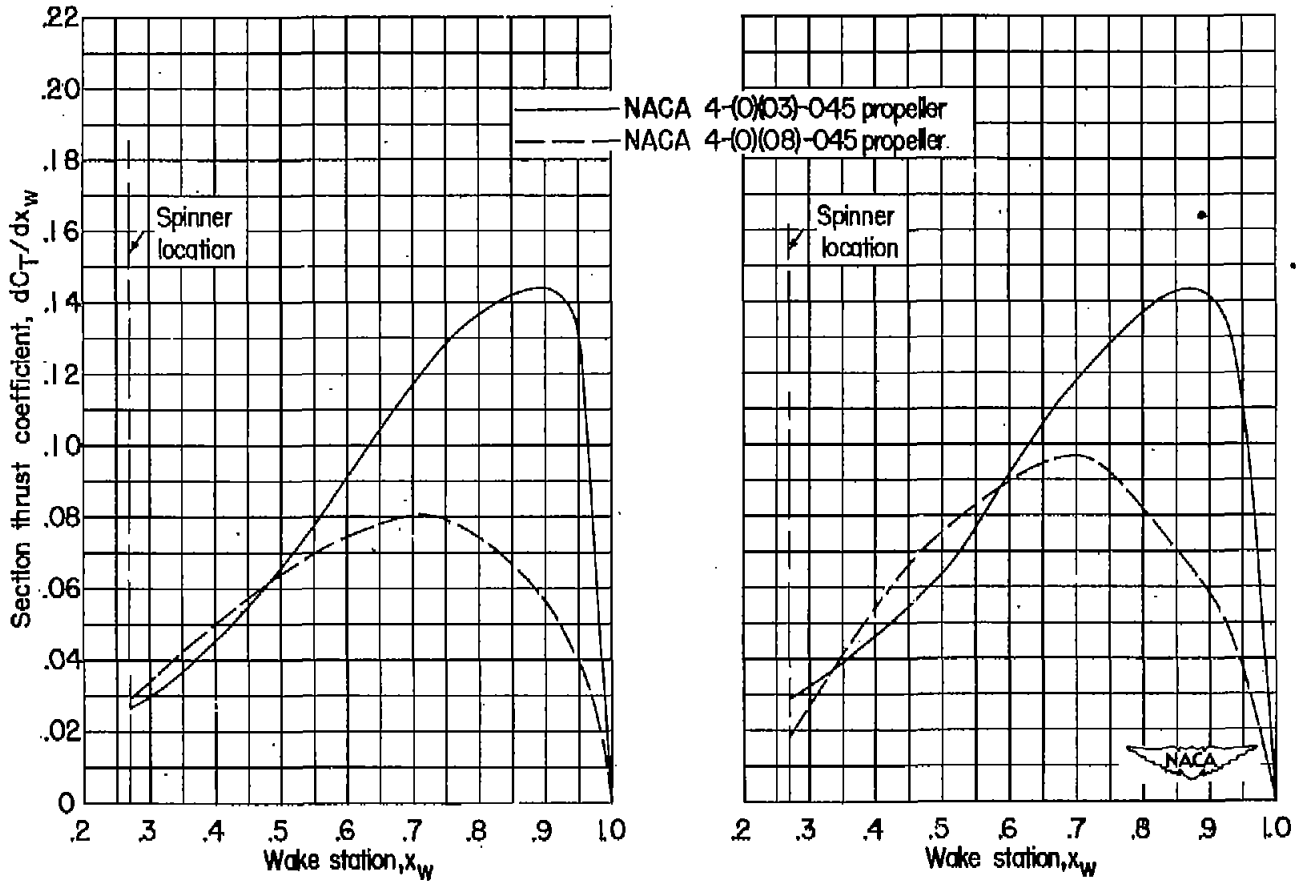

(a) M = 0.65. (b) M = 0.70.

Figure 11.- Effect of thickness ratio on section-thrust-coefficient curves at constant advance ratio. $J = 3.7$; $\beta_{0.75R} = 60°$.

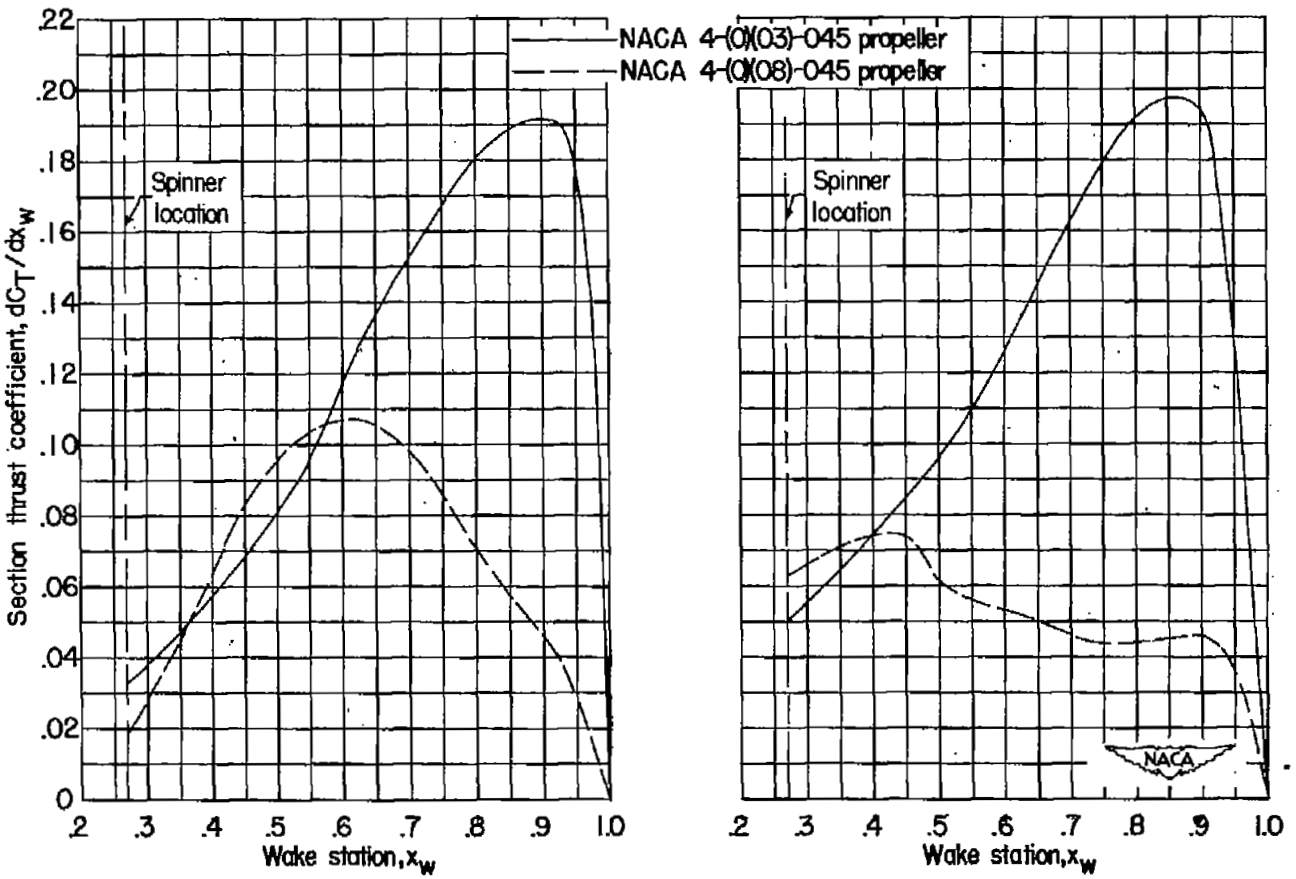

(c) M = 0.75.

(d) M = 0.80.

Figure 11.- Continued.

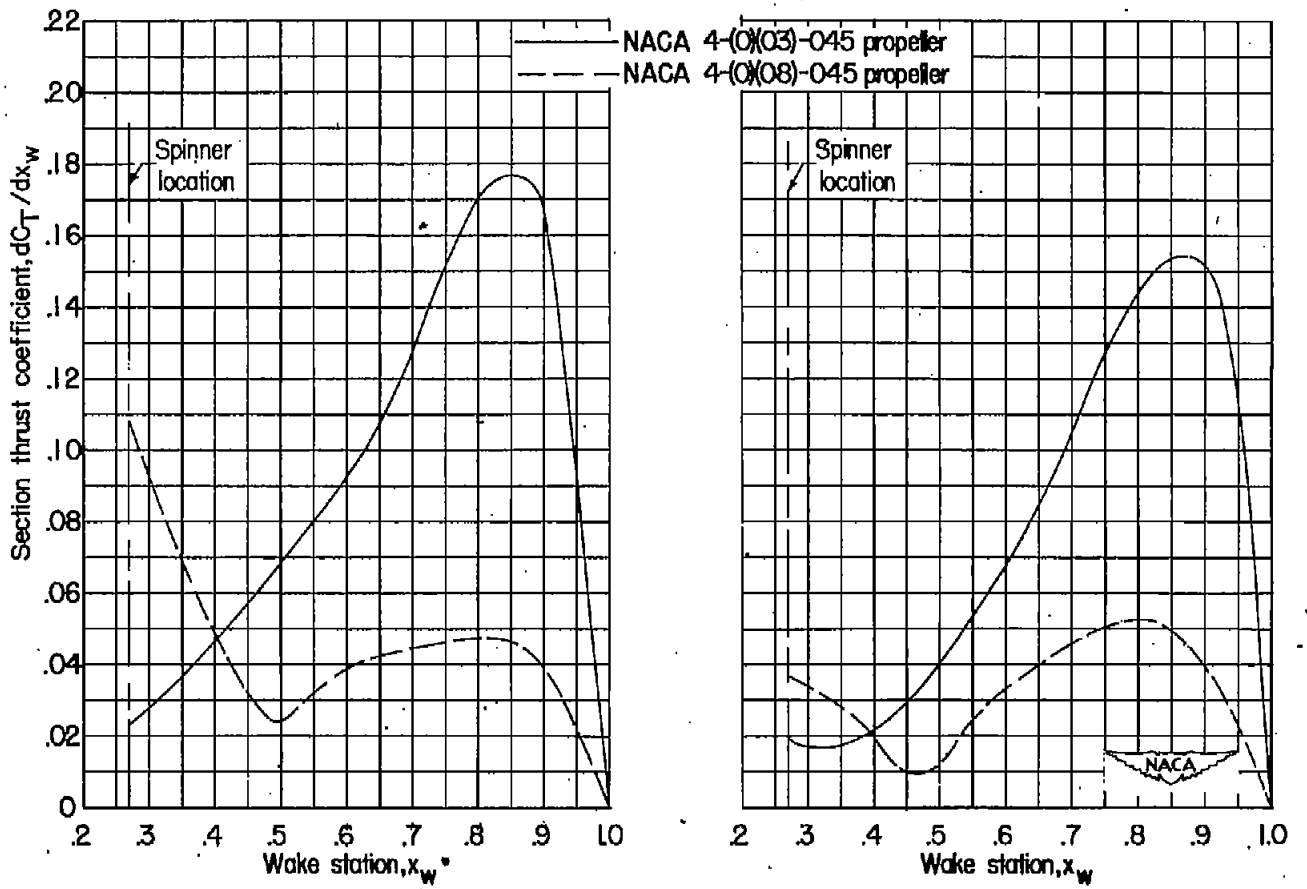

(e) M = 0.85. (f) M = 0.90.

Figure 11.- Concluded.

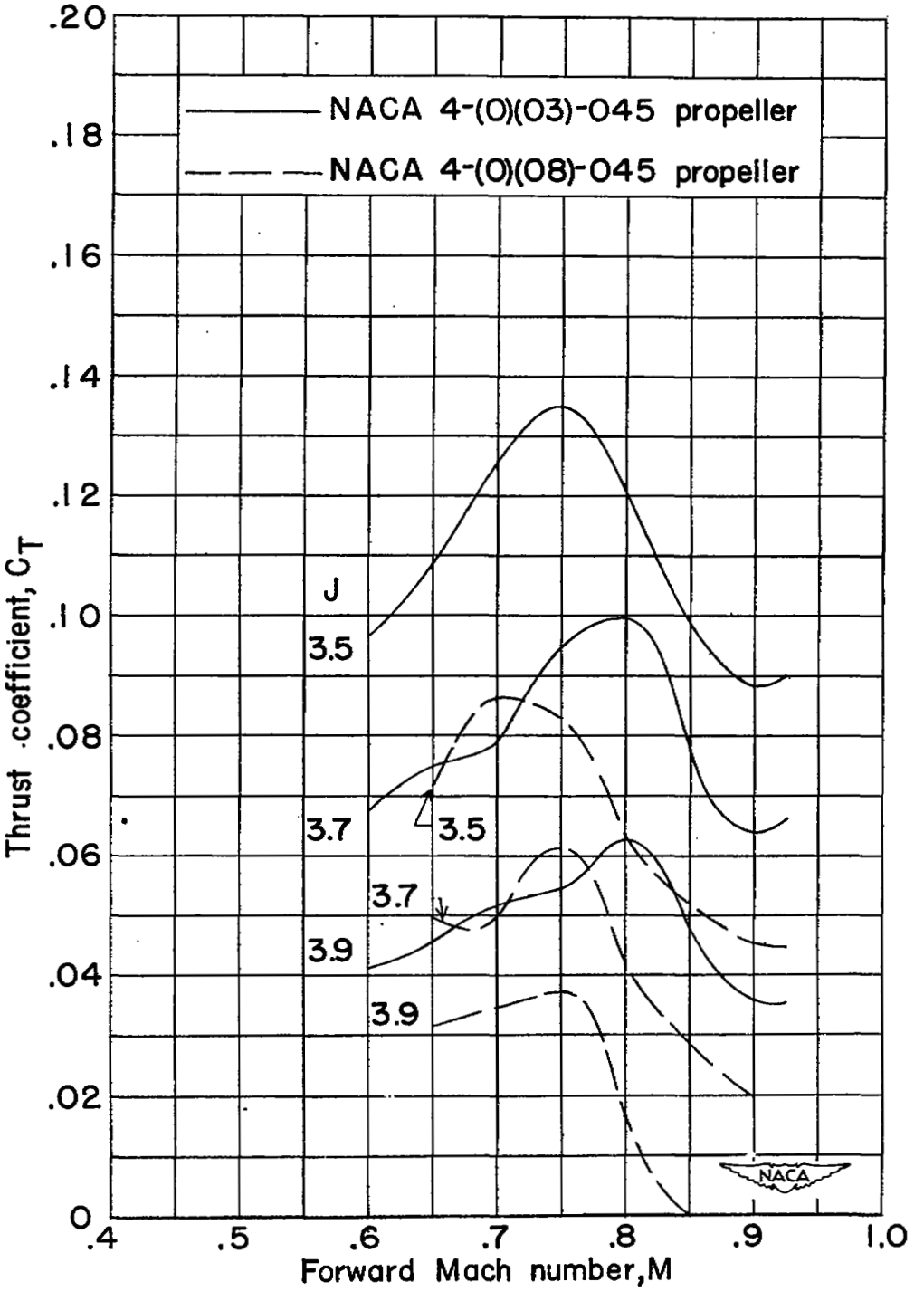

Figure 12.- Effect of thickness ratio on thrust coefficient.